

ARB-valsede laminatkompositter av AA3103 og Cu

Jan Gaute Frydendahl

Materialteknologi

Innlevert: Juni 2012

Hovedveileder: Bjørn Holmedal, IMTE

Medveileder: Nagaraj Vinayagam Govindaraj, IMTE

Norges teknisk-naturvitenskapelige universitet
Institutt for materialteknologi

TMT4905 Master's thesis

June 2012

**Multilayered composites of AA3103 and Cu
produced by Accumulative Roll Bonding (ARB)**

Jan Gaute Frydendahl

Supervisors:

Professor Bjørn Holmedal

PhD stipendiat Nagaraj Vinayagam Govindaraj

Department of Materials Science and Engineering



NTNU – Trondheim
Norwegian University of
Science and Technology

Preface

I, Jan Gaute Frydendahl, hereby declare that the writing of this master's thesis and its corresponding research work has been performed independently and in accordance with the regulations at the Norwegian University of Science and Technology, NTNU.

This report has been developed from January 2012 to June 2012 at the Department of Materials Science and Engineering, NTNU, under the supervision of Professor Bjørn Holmedal and PhD stipendiat Nagaraj Vinayagam Govindaraj. I would like to extend my deepest gratitude for the outstanding theoretical and practical help my supervisors have granted me during both this semester and the previous project work.

Furthermore, I would like to thank Pål Skaret for help with the tensile testing and flexural tests, Yingda Yu for practical advice during SEM sessions, Robert Karlsen at Finmekanisk verksted for machining lots of test specimens, and to the guys at the workshop for letting me use their cutter.

Trondheim 15th of June 2012

Jan Gaute Frydendahl

Abstract

Laminate composites have been made out of sheets of aluminum AA3103 + copper, and AA3103 + brass C24000 utilizing an accumulative roll bonding (ARB) technique. Two different copper/aluminum preforms were subjected to up to 6 passes of roll bonding at 350°C while retaining continuous layer structure throughout the process, although the relatively low degree of cold working yielded little to none strength gain. 3 other parallels of preforms were made of copper, non-annealed brass, and annealed brass, stacked between two significantly strained, cold rolled aluminum sheets. The first pass of ARB for each parallel was performed at 350°C, while consecutive passes were performed at room temperature (CARB). Every specimen created via this process route was severely cracked, along the middle of the sheet in the rolling direction, during the 5th pass of ARB. In addition, the large, accumulated strains caused substantial cracking at the edges of the sheet.

Prior to cracking, the cold rolled specimens showed an increase in strength with increasing amount of cold working as long as the copper/brass layers were continuous. As soon as these layers fractured, and the copper/brass layers turned discontinuous, the materials showed a significant reduction tensile strength, flexural strength, and homogeneity among test specimens taken from different areas of the samples.

Earlier research work has stated that differences in plastic flow may cause instabilities at the interfaces, leading to necking of layers of the harder material, and sheet thickness of the preform stacks were balance to counteract this mechanism. However, the samples produced during the work described in this report showed another, hitherto overlooked, instability mechanism contributing to deformation of the layers: shear deformation. Shear bands were discovered in the copper layers during EBSD investigations, and presumably corresponding wave-like deformation patterns were observed in light optical microscope, propagating between layers.

Further ARB cycles of the investigated materials would not be possible without some kind of intermediate heat treatment granting relaxation to the greatly hardened materials.

Contents

Preface	I
Abstract	II
Contents	III
1 Introduction	1
2 Theory	3
2.1 Cold rolling.....	3
2.2 Roll bonding.....	4
2.2.1 Surface preparation for roll bonding.....	4
2.3 Accumulative roll bonding.....	5
2.3.1 The ARB process.....	6
2.3.2 Control of layer continuity.....	6
2.4 Hall-Petch strengthening.....	9
2.5 Material properties.....	10
2.5.1 Recrystallization behavior of Cu.....	10
2.5.2 Recrystallization behavior of AA3103.....	12
2.6 Tensile testing.....	12
2.7 Three point flexural testing.....	13
3 Experimental methods	15
3.1 ARB.....	15
3.2 Light optical microscopy.....	19

3.3 Tensile testing.....	19
3.4 Three point flexural test.....	20
3.5 EBSD.....	21
4 Experimental results.....	22
4.1 ARB specimens.....	22
4.2 Light optical micrographs.....	22
4.3 Tensile test results.....	28
4.4 Three point flexural test results.....	37
4.5 EBSD results.....	41
5 Discussion.....	44
5.1 Micrographs.....	44
5.2 Tensile tests.....	45
5.3 Flexural tests.....	46
5.4 EBSD images.....	47
5.5 Instability mechanisms.....	47
6 Conclusion.....	48
7 References.....	49
Appendix A: Measured thicknesses of the machined samples.....	50

1 Introduction

When sub-micrometer, or even nano-scaled, thickness of the layers in metallic multi-layered composites is achieved, these materials have shown improved mechanical, electrical, and magnetic properties. Metallic multilayers have earlier been produced using ion sputtering, vapor deposition techniques, and other methods that create the layers one by one [1]. Roll bonding is a form of welding by rolling that has been known for several decades. However, it has recently been subject to a renewed research interest as a way of producing ultra-fine layered materials by a top-down approach. Accumulative roll bonding (ARB) is an iterative process, where each repeated pass of roll bonding yields finer layer- and microstructure of the rolled material (Fig. 1.1). Compared to the bottom-up methods, this is an economically beneficial and relatively simple process, with greater possibilities of expanding into an industrial scale of production volumes.

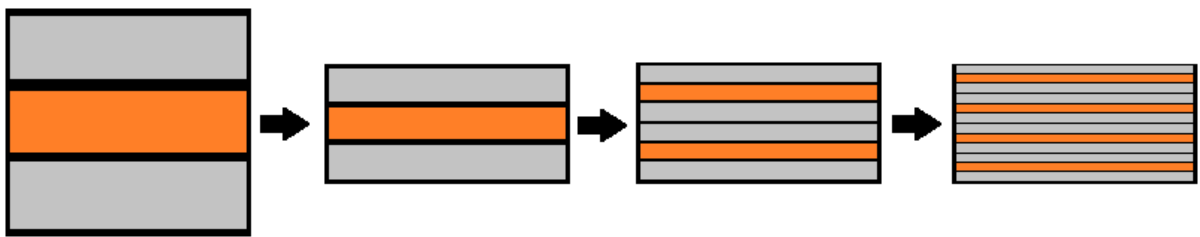


Figure 1.1: An illustration of the layer structural evolution of a bimetallic ARB composite with 50% reduction during rolling. From left to right: Non-rolled preform, after 1, 2, and 3 passes of roll bonding. The initial three sheets shown are just one example of many possible starting combinations.

However, there are some major challenges with the ARB process. Especially when it comes to retaining structural and mechanical integrity of the material as the degree of accumulated cold working increases. When roll bonding dissimilar metals, difference in plastic flow will cause instabilities at the interfaces, leading to premature necking and fracturing of the layers. Another challenge with accumulated cold working is that work hardening metals will become increasingly more hard and brittle as the number of passes increases, leading to severe

fracture growth along the rolling direction of the material during rolling. In all roll bonding processes, the surface preparation prior to the actual pressure welding is critical for maximizing bond strength, or for bonding to happen at all.

The focus of the work depicted this report is on production methods, structural analysis, and the mechanical properties of multi-layered composites for two kinds of bimetals, while attempting to address the challenges mentioned in the previous paragraph. The two groups of bimetallic laminate composites consist of aluminum (AA3103) + copper (commercially pure) and AA3103 + 80/20 brass (C24000). For comparison with more conventional construction materials, and a monometallic alternative, a parallel consisting of several sheets of AA3103 only was included in the research.

Researchers have published work proposing that Cu in an Al/Cu layered composite will neck and fracture before nano-scale is reached. However, it has also been suggested that the layer continuity can be kept down to sub-micrometer thickness, and no research testing this limit has been found prior to this work [2].

2 Theory

2.1 Cold rolling

As a method of cold working materials, cold rolling (CR) results in higher strength and lower ductility compared to the material's properties prior to deformation. During rolling, the grains in the microstructure of the metal become elongated along the rolling direction. Severe plastic deformation (SPD) causes subdivision of grains into an ultrafine grained (UFG) lamellar structure with the long sides of the boundaries parallel to the rolling direction. [5, 6]

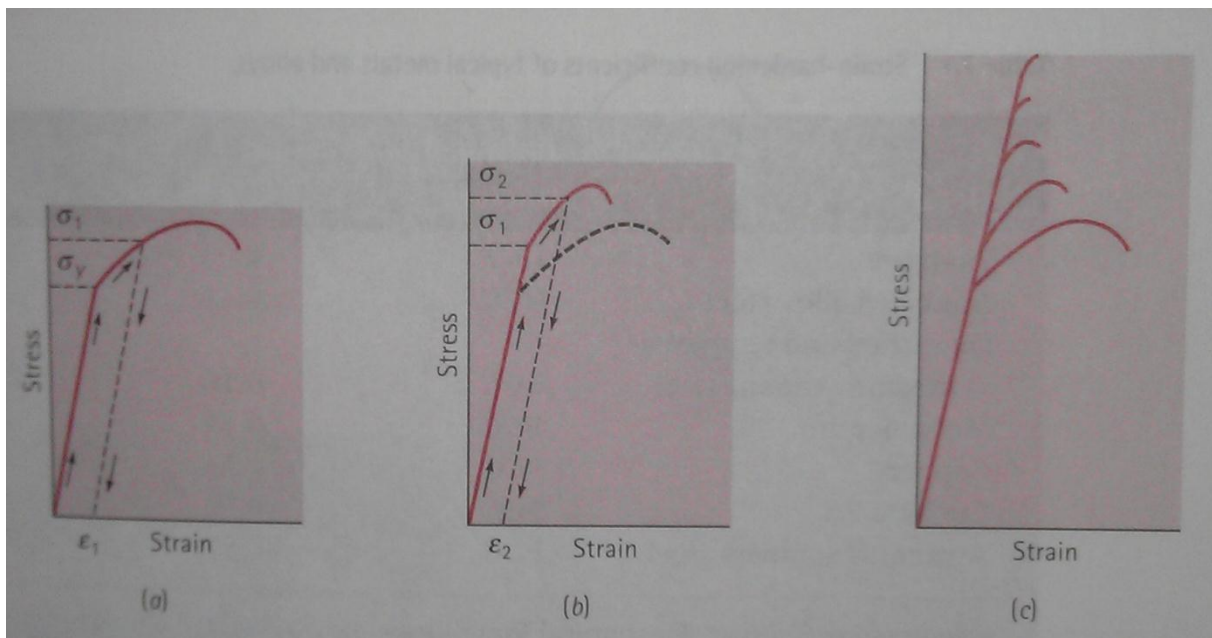


Figure 2.1: Engineering stress/strain curves showing evolution of the strength of a cold worked material. a) Shows the curve for the non-deformed material. b) Shows the curve after the effect of the cold working illustrated in a). c) Illustrates the accumulative effect of repeated cold working [6].

2.2 Roll bonding

Roll bonding is a type of cold welding by pressure, where metal sheets form a bonded interface during rolling. The oxide layers of the metals come into contact and break up as a brittle layer during rolling. In the cracked areas of the oxide layer, the exposed virgin metal of the two metal sheets are brought into atomic contact with each other while being subject to high pressure, and this will under the right circumstances create a bonded interface. Since the oxide layers can, in practice, be considered completely brittle, the area available for bonding is equal to the increase in area of the interface, and the strength of the bonding can then be assumed to increase with increasing deformation (thickness reduction). Other factors that have been found to promote bond strength are: increased pressure, increased temperature, increased mill diameter and decreased roll speed [5, 6]. For laminates of dissimilar metals, higher bond strength leads to larger uniform deformation of the material, as the interface will constrain and delay necking of the Cu-layers [7].

2.2.1 Surface preparation for roll bonding

For bonding to happen, and to maximize bond strength, the surfaces of the metal sheets have to be cleaned and mechanically prepared. As shown in figure 2.2, taken from investigation [6], the best of the previously tested methods is to clean the surfaces with a degreasing agent, followed by mechanical brushing. Scratch brushing prior to degreasing is proven to be a less beneficial procedure. This is probably because the brush may press the contaminants into the uneven surface, making degreasing less efficient. The cleaning removes grease and other impurities, while the brushing creates a work hardened layer with topography. That layer promotes bonding by making the work hardened layers stick to each other and break up as one during rolling. The heat from the mechanical working will also remove some adsorbed contaminants from the surrounding air, such as condensed water vapor, assuming that prolonged exposure to atmosphere after brushing is avoided. Rolling at sufficiently elevated temperatures will also remove this kind of impurities [6].

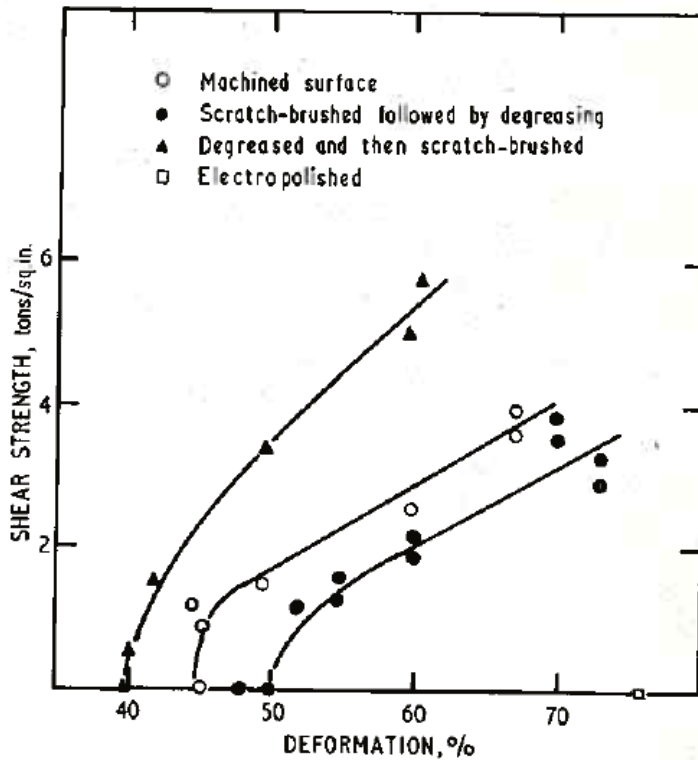


Fig. 2.2: Bond strength of different surface preparation techniques vs. degree of deformation [6].

2.3 Accumulative roll bonding

Accumulative roll bonding is the process of repeated roll bonding of the same specimen, giving a number of layers in the material that grows exponentially with the number of completed cycles. The process was invented in 1998, by Saito et al., as a way of fabricating bulky, ultrafine grained (mean grain size smaller than 1 micron) materials by a process involving severe plastic deformation (SPD). Other SPD processes, like equal channel angular extrusion/pressing (ECAE/ECAP) and high pressure torsion (HPT), lack either the possibility of creating ultrafine grained structure, or have limited total thickness of the products [8]. As the number of layers is doubled with each pass, the number of layers in the composite material is equal to the number of initial layers times $2^{(n-1)}$, where n equals the number of passes through the roll mill during the ARB process.

2.3.1 The ARB process

First, a preform is made from a stack of two or more sheets of metal. After an initial pass through the roll mill, the sample is cut into two equally sized pieces. These pieces are then given the same surface preparation treatment as the initial sheets, and are then stacked and rolled again. This process can be repeated for any number of passes. As long as the harder phase exists as continuous layers, the thickness will continue to refine during each cycle. When necking and fracture of the harder metal occurs, the resulting material will consist of homogeneously distributed particles in a matrix of the softer metal. At this point, the harder metal will affect the strength of the composite through particle hardening.

The difference between conventional cold rolling and ARB is that the mean angular misorientation between the grains in the rolled sheet is larger for ARB samples, leading to a faster formation of the ultra-fine grained (UFG) structure compared to conventionally rolled samples. A potential reason for this difference is redundant shear strain distributed among the previously bonded interfaces across the cross-section of the ARB composite [8]. Furthermore, ARB opens up the possibility of stacking different materials, as other welding techniques may not allow dissimilar metals to be joined.

2.3.2 Control of layer continuity

According to Lee et al. [2], the combination of metals in bimetallic multilayers can be divided into two main groups. In one, the hardest layers neck and rupture into lamellae during the deformation process. In the other, the continuity of the layers is maintained until the thickness reduction reduces the layers to nano-scale. Even though the Al/Cu-combination is suggested to belong to the former case, bimetals of this composition may elongate down to UFG structure after necking occurs [1]. Reaching minimum layer thickness for a combination of materials may be dependent on finding the optimal annealing treatment for recovery at various stages in the process.

In the investigation conducted by Eizadjou et al. [1], a copper layer thickness of $6.94\ \mu\text{m}$ was achieved with no intermediate annealing and rolling at ambient temperatures (Fig. 2.3), although these layers were discontinuous, and fractured at an early stage in the process. An example of an ARB material with nano-scaled, continuous layers is the Fe/Ag laminate shown in fig. 2.4. This material, however, was annealed three times at 600°C for 1h during the process, and the differences in recovery rates made the initially soft Ag take over as the harder layers as the Fe recovered to a greater extent during annealing, making the flow rates of the materials approach one another, leading to approximately uniform layers in the final sheet. In addition, the manufacturing method differed somewhat from the ARB process, as the actual bonding occurred while being hot pressed in vacuum, at 300°C , and subsequently rolled for several passes to 90% reduction at room temperature.

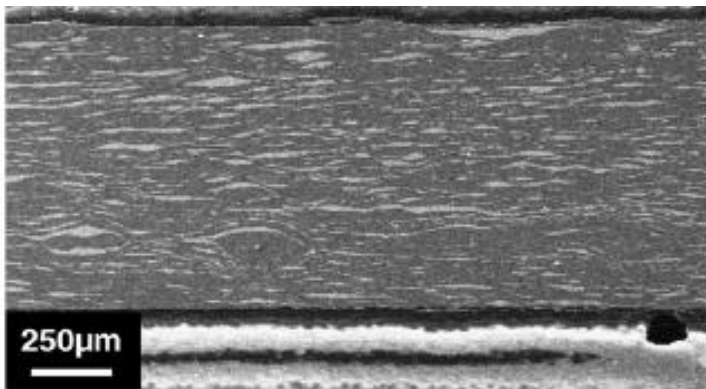


Figure 2.3: SEM micrograph of an ARB Al/Cu composite cold rolled for 5 passes [1].

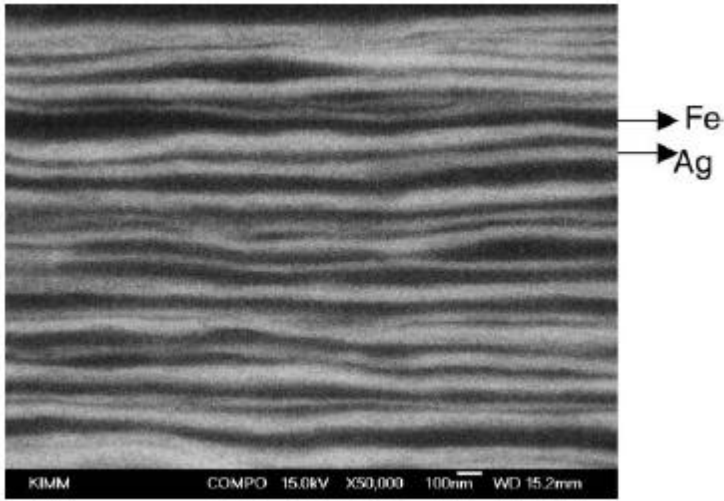


Figure 2.4: SEM backscatter micrograph of Fe/Ag sheets [2].

Differences in flow properties of the phases cause a plastic instability that is magnified by the stress concentration around necks in the hard layers. The elongation between necking and fracture is determined by the differences in flow characteristics of the metals and the work hardening rate of the soft phase, as this phase has to counteract further deformation in the area surrounding the neck.

According to [8], the critical equivalent strain and critical thickness reduction for necking can be determined by the following relations:

$$\varepsilon_c \geq \frac{n_h}{\sqrt{3}(1-H) \left(1 - \frac{k_s}{k_h} \varepsilon_c^{n_s - n_h}\right)} \quad (2.1)$$

$$r_c = 1 - \exp\left(-\frac{\sqrt{3}}{2} \varepsilon_c\right) \quad (2.2)$$

ε_c : Critical equivalent strain

r_c : Critical thickness reduction

H: Initial thickness ratio of the hard layer to the total thickness of the material.

n: Strain hardening exponent (Subscript “s” for soft layer and “h” for hard layer).

k: Strength coefficient (Subscript “s” for soft layer and “h” for hard layer).

The critical reduction for necking is increased with increasing initial thickness ratio of the hard phase. These equations are only valid for materials in which necking occurs.

2.4 Hall-Petch strengthening

When plastic strain is applied to a metal, dislocations glide within the polycrystal's grains. Grain boundaries are impenetrable to these dislocations, as the angular mismatch between the crystallographic orientations of the grains impedes further gliding. However, at a certain critical shear stress, the pile-up of dislocations can trigger dislocation sources and dislocation generation in neighboring grains. A large number of dislocations in the pile lower this critical stress, as each dislocation contributes to overcoming this barrier. In a fine grained microstructure, the number of dislocations that one grain can contain is limited, and the stress for continued deformation becomes higher. Equation 2.3 is named the Hall-Petch relation, and can be used to calculate the value for the yield stress when the grain size of the material is sufficiently low to give Hall-Petch strengthening [3].

$$\sigma_y = \sigma_0 + \frac{k_y}{\sqrt{d}} \quad (2.3)$$

d: Mean grain size

k_y : Strengthening coefficient unique to each material

The Hall-Petch relation is only valid down to grain sizes of about 10 nm. Below this size, the prevented dislocation glide becomes irrelevant, as grain boundary sliding occurs [3].

2.5 Material properties

The materials used for creating ARB sheets during this work are commercial pure copper, C24000 low brass (80/20), and AA3103 aluminum. As the temper designations and equivalent degrees of cold working of the obtained copper materials were unknown, the data listed in the following table contains typical values for similar, representative materials. For brass, the data found for OS025 temper is similar to the results found during tensile testing. The data listed for copper is for annealed 100% pure copper. The standard with the highest degree of cold working found for sheets of AA3103 is the purely strain hardened H18 condition, and has been included for comparison reasons only, as the sheets used in the preform stacks are strained even further, having at least 50 MPa higher ultimate tensile strength than the shown example. All values are given for standard pressure and temperature.

Table 2.1: Material properties.

	Pure copper [9]	C24000 brass [9]	AA3103 [10]
Condition	Annealed	OS025	H18
Density	8.93 g/cm ³	8.67 g/cm ³	2.74 g/cm ³
Tensile Strength, Ultimate	210 MPa	330 MPa	200 MPa
Tensile Strength, Yield	33.3 MPa	115 MPa	185 MPa
Elongation at Break	60.00 %	47.00 %	7 %
Modulus of Elasticity	110 GPa	110 GPa	-

2.5.1 Recrystallization behavior of Cu

Figure 2.5 shows fractional softening for 99.95% pure copper at isothermal annealing after cold rolling at an equivalent strain of 3.7 mm/mm. The results show that copper recovers from heavy cold working even at room temperature. When rolling ARB materials at 350°C it is reasonable to assume that the fractional softening will have significant impact on the properties of the Cu layers in the samples after 10 minutes of exposure. Furthermore, fig. 2.6 displays results from “An Ohno continuous casting (OCC) round bar of pure copper (99.99%) with a diameter of 8 mm” deformed to 10% strain at different strain rates. The bars were then kept in isothermal environments of four different temperatures for 7 days with an extensometer attached. At the higher strain rate, closest to the one experienced by the one

experienced by the ARB rolled sheets, it is shown that pure copper recovers between 0.04 and 0.05% strain after 7 days [11]. Alloying elements, such as the zinc in brass, would presumably slow down these mechanisms.

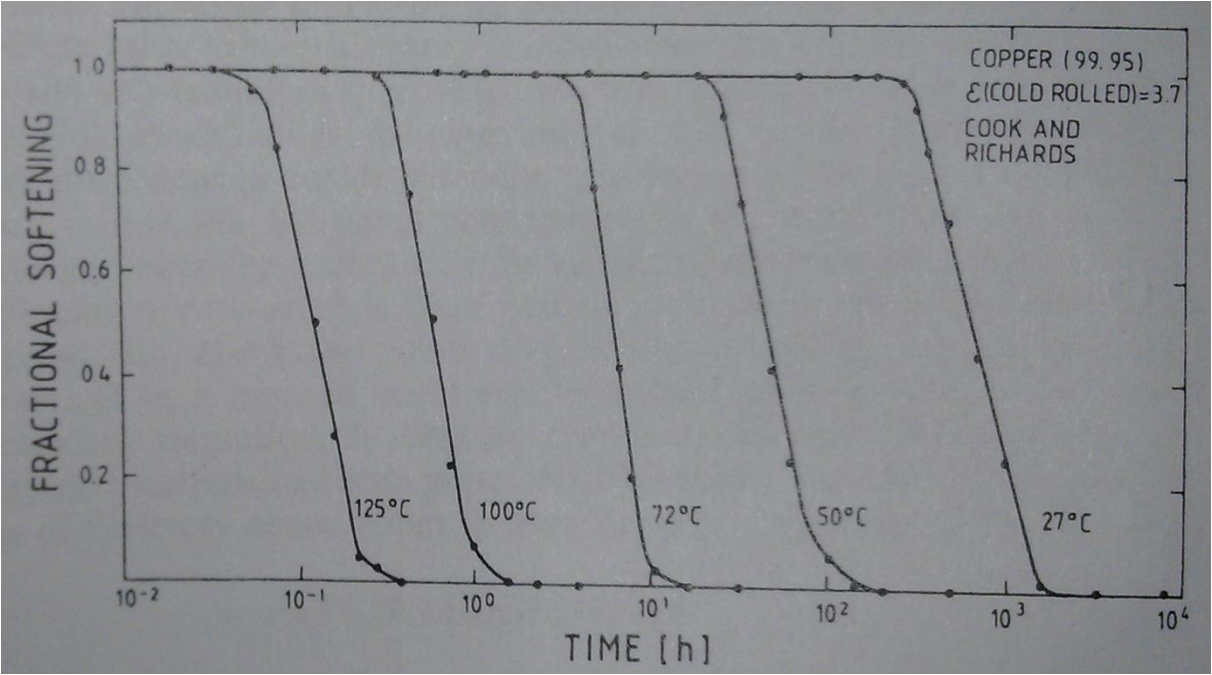


Figure 2.5: Fractional residual strain hardening curves for isothermal annealing of copper.

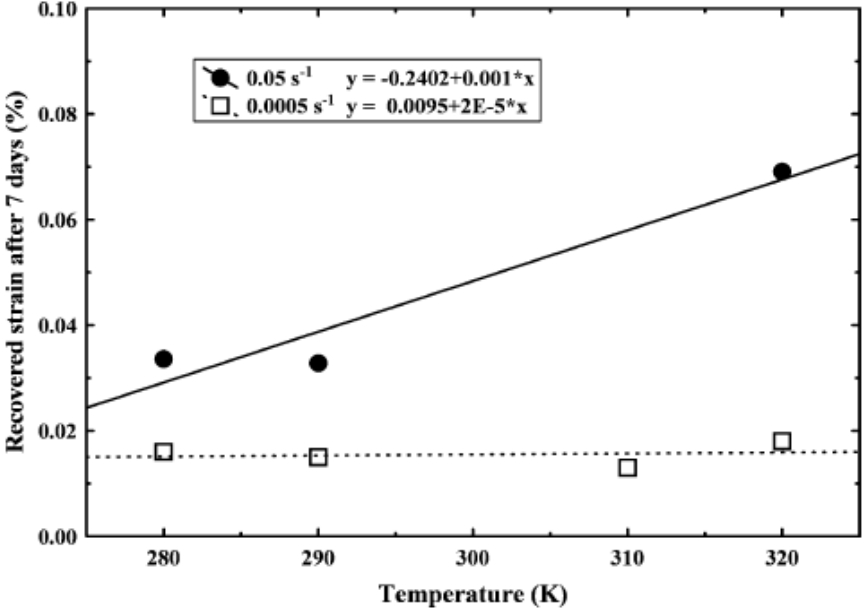


Figure 2.6: Isothermally recovered strain in pure copper strained to 10% elongation [11].

Copper and brass materials are often given different temper designation to indicate what amount of cold working, tempering, or annealing treatment the material has been subject to. H00-H14 indicates cold working and tempering, with increasing amount of equivalent strain. The H50-H90 range contains different forming techniques. Designations O10-O82 are given to annealed materials, while OS005-OS200 are given to materials annealed to 0.005-0.2 mm average grain size [12].

2.5.2 Recrystallization behavior of AA3103

AA31XX alloys are often annealed at 345°C [13]. Heating to 350°C for 10 minutes would cause some amount of relaxation in heavily cold worked sheets. For ARB AA3103 materials, Haaland showed that ARB sheets rolled to a tensile strength of approximately 280 MPa would drop to about 250 MPa tensile strength after 600 seconds ([14] Fig. 59, p. 52).

2.6 Tensile testing

For tensile testing, machined samples of known geometry are attached in both ends to a hydraulic or electromagnetically driven machine. The cross-heads that hold the specimen separate at a known, constant speed, and the force applied to the material is measured. An extensometer simultaneously measures the elongation of the narrow test area of the sample. Since initial the cross-sectional area is known, the applied pressure can be calculated from this, and the results are displayed in a plot of engineering stress vs. engineering strain.

The engineering stress is defined as:

$$s = F/A_0 \tag{2.4}$$

Where F is the applied force, and A_0 is the initial cross-sectional area. The elongation is defined as:

$$e = \Delta l/l_0 \tag{2.5}$$

Where l is the length of the extensometer at the applied load, and l_0 is the original gauge length before load was applied to the sample.

2.7 Three point flexural testing

Flexural testing, also known as bend testing, is frequently applied to brittle materials, like ceramics, as a way of determining the material's strength, or to determine bendability of more ductile materials. This method can also be applied to laminate composites to investigate interface bond strength and crack propagation through the layers of the material.

In a three point flexural test, the specimen is placed on two fixed support rolls with a known span. A third, mobile roll is then lowered to the sample surface midway between the support rolls. The surface is then calibrated as the zero-point for deflection measurement. During testing, the middle roll is lowered at a constant rate, applying force to the specimen until failure, or a predetermined displacement, is achieved [4]. The force and displacement are measured, and the flexural stress for a rectangular cross-section is given by:

$$\sigma_f = \frac{3PL}{2bd^2} \quad (2.6)$$

σ_f : Flexural tensile stress at outer surface (MPa).

P: Measured force (N).

L: Span between supporting rolls (mm).

b: Width of specimen (mm).

d: Thickness of specimen (mm).

During bending of the sample, the outer surface will stretch, and the inside surface will be in compression, as illustrated in fig. 2.7. If the compression is equal to the tension, the center line through the cross-section would be in a stress neutral state (fig. 2.7a). In practice,

however, the outer surface will be strained more than the inner part is compressed. This leads to thinning of the outermost part of the material, and the neutral line will be shifted inwards, as shown in fig. 2.7c [15].

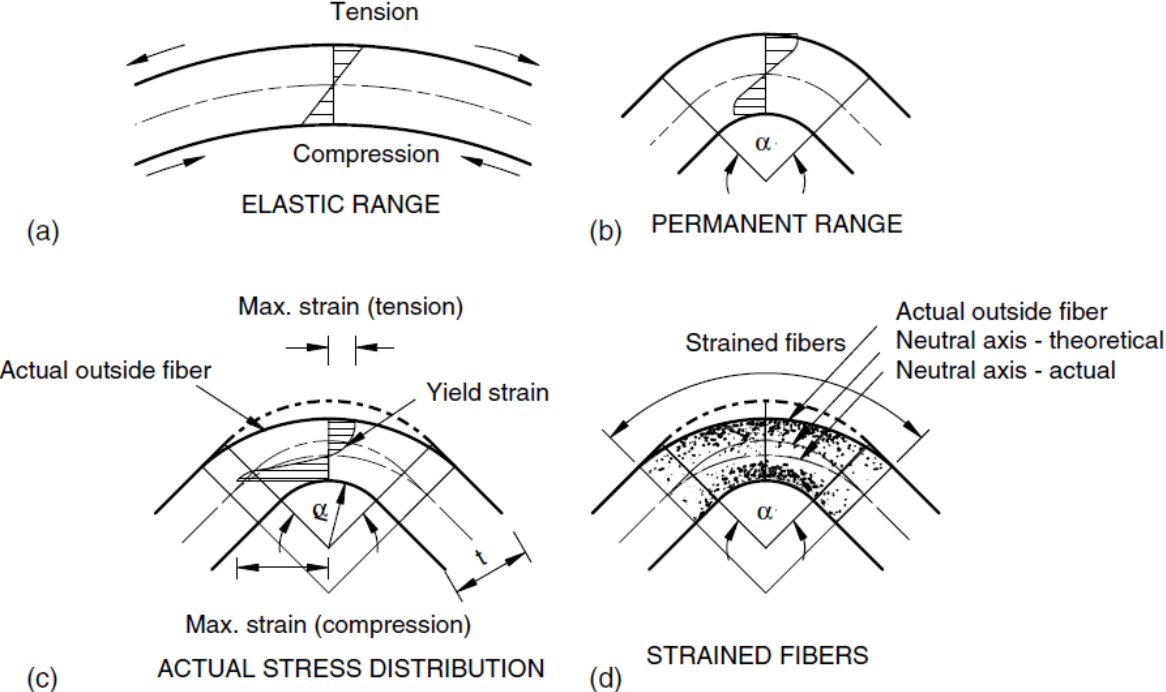


Figure 2.7: Tension-compression distribution during bending of metallic specimens [15].

3 Experimental methods

3.1 ARB

Six different types of preforms were made of sheets of AA3103, C24000 brass (80/20), and commercial pure copper. The aluminum was rolled down from homogenized blocks of 20 mm thickness down to sheets of 1 mm and 0.5 mm thickness through several passes of rolling. No heat treatment was applied prior to roll bonding, apart from heating to rolling temperature.

The Cu was taken from rolled sheets of 1 mm commercially pure copper, as purchased from factory. Initial degree of cold working for this material is unknown. Likewise, the brass was used as purchased; rolled sheets of 1 mm thickness. The supplier didn't list any temper designation for the brass, so any consecutive heat treatment of this material after factory rolling is unknown.

The sheets were cut into pieces measuring 220 x 40 mm. The length was limited by the depth of the oven used for heating to rolling temperature, and the width of the sample had to be scaled according to the operating pressure of the rolling mill.

One set of copper preforms consisted of one copper piece and one 1 mm thick aluminum piece, while the second group of specimens was made up of one copper sheet stacked between two 1 mm sheets of aluminum. This gives an H-ratio (equation 2.1) at a value of 0.5 for the Al/Cu samples, and 1/3 for the Al/Cu/Al samples. The Al/Cu gives an asymmetric composite, where copper bonds to aluminum each pass, and the Al/Cu/Al configuration yields symmetric samples where aluminum bonds only to aluminum beyond the first pass. These samples were heated to 350°C for 10 minutes and rolled as fast as possible after leaving the oven for 2, 4 and 6 passes. The third set of copper materials contained stacks of two aluminum sheets of 0.5 mm and one sheet of 1 mm copper in an Al/Cu/Al sequence. This third parallel had an H-ratio of 0.5, and was rolled at 350°C for the first pass, to ensure successful bonding and

maximizing bond strength when bonding of dissimilar metals occurs (Higher temperatures ensure higher bond strength, as described in section 2.2). Furthermore, 2nd, 3rd, 4th and 5th pass samples were rolled at room temperature. The different starting stacks are shown in figure 3.1.

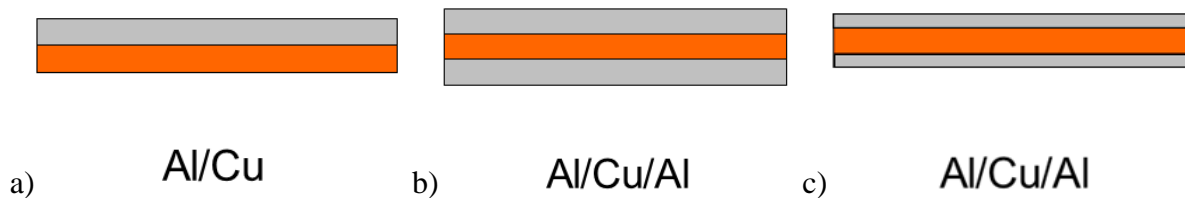


Figure 3.1: Illustration of the three different starting stacks for production of the ARB samples containing copper.

Two parallels of brass samples were made of the same stacking dimensions as illustrated in fig. 3.1 c), with 1 mm brass between 0.5 mm sheets of AA3103. One set of stacks contained the brass as purchased. This material was presumed to have a temper designation in the H00-H14 range (See section 2.5.1). The other set consisted of brass that was annealed for 1 hour at 600 °C and then quenched in room tempered water. As with the cold rolled Al/Cu/Al sample, only the first pass was performed at 350 °C, and the following passes of ARB were conducted at room temperature. Samples were made at 1, 2, 3 and 4 passes.

Further rolling of the cold rolled specimens resulted in sheets that were severely cracked and split along the middle of the length axis of the rolled piece. Those specimens were not suited for machining of test samples, and were thus not included in the characterization work.

As a means of comparing the Al/Cu composites to identically treated materials of aluminum, a final group of materials were made out of aluminum sheets only. One sheet of 1 mm thick aluminum was stacked between two sheets of 0.5 mm thick aluminum and rolled for 1, 2, 3 and 4 passes. The rolling temperature was 350 °C for the first pass, and room temperature for the consecutive passes. Throughout this report, the designation CARB (Cold ARB) will be

used to refer to these samples. This designation includes first pass of roll bonding at 350 °C. An overview of the different parallels is given in table 3.1.

Table 3.1: Overview of all samples produced.

Name	Composition	Heat treatment	Number of passes
Al/Cu	1 mm Al / 1 mm Cu	Rolling at 350 °C	2, 4, 6
Hot Al/Cu/Al	1 mm Al / 1 mm Cu / 1 mm Al	Rolling at 350 °C	2, 4, 6
CARB Al/Cu/Al	0.5 mm Al / 1 mm Cu / 0.5 mm Al	1 st pass at 350 °C	1, 2, 3, 4, 5
NA Al/Br/Al	0.5 mm Al / 1 mm brass / 0.5 mm Al	1 st pass at 350 °C	1, 2, 3, 4
Annealed Al/Br/Al	0.5 mm Al / 1 mm brass / 0.5 mm Al	Annealed 1 hour at 600 °C. 1 st pass at 350 °C	1, 2, 3, 4
3*Al	0.5 mm Al / 1 mm Al / 0.5 mm Al	1 st pass at 350 °C	1, 2, 3, 4

The surfaces that were to participate in the bonding process were degreased in acetone and scratch brushed with a wire brush of 0.3 mm diameter strands. The brush was attached to a FLEX LE 14-7 125 INOX angle grinder revolving at a speed of 3800 rpm. The samples were then riveted in both ends with aluminum rivets and a rivet gun, to prevent sliding of the surfaces relative to each other during rolling. The hot rolled specimens were heated to 350°C for 10 minutes in an oven, before being rolled to 50% thickness reduction on a two-high hydraulic rolling mill. The samples that were rolled at room temperature were rolled within 2 minutes of brushing, to limit the amount of reformed oxides and condensed contaminants on the surfaces [6]. This process was repeated with each pass for all compositions. The roll gap had to be adjusted by measuring the thickness of rolled dummy pieces, without any means of measuring accurately. In addition, the amount of elastic recovery changed with different layer structures and number of passes. These factors lead to variations in the thickness of the specimens after rolling, but all the samples ended up in close approximation to the target thickness. The actual, measured thicknesses can be found in appendix A.



Figure 3.2: Photograph of the wire brushing equipment and a partially brushed aluminum sheet.

To remove the rivets and thereby prevent them from further affecting the material, the ends of the samples were cut off between each pass. The edges of the samples were trimmed when the edge cracks started growing, to avoid severe crack propagation. As a consequence of this, the samples had very limited size at a higher number of passes. To enable the production of samples with a large number of passes, while maintaining an adequate sample size, pairs of identically treated samples were combined at various steps in the process.

Since the steel rolls in the roll mill itself were at room temperature during rolling, the specimens rolled at an elevated temperature experienced rapid cooling during rolling, and will have experienced some amount of cold deformation after leaving the oven. The hot rolled materials were reheated to 350°C prior to each pass through the roll, and at least some of the earlier cold working would be negated by this heat treatment.



Figure 3.3: The two-high hydraulic rolling mill used for roll bonding.

3.2 Light optical microscopy

The samples were molded into an acrylic resin (ClaroCit), with the cross-sectional cut parallel to the rolling and normal directions. The specimen surfaces were grinded flat with abrasive paper of 320, 500, 800, 1200, and 2400 grit, and then polished with discs infused with diamond particles of 3, 1, and 0.25 micron diameter. Micrographs were taken at 50 and 1000 times magnification.

3.3 Tensile testing

Tensile testing of the materials was performed with MTS 810 material testing equipment, where the specimens are mounted in two clamp-like cross heads. Upon starting the testing program, one of the heads begins moving at a constant rate, while applied force is measured, stress is calculated from manually entered dimensions by the attached software, and elongation is measured by an elastometer attached to the outer regions of the test area of the

sample. Machined, flat test samples of the ARB materials were tested in uniaxial tension until failure, and compared to similarly dimensioned tensile samples taken from the copper, brass and aluminum sheets from the original preforms. The length of all the samples was oriented as close to parallel to the rolling direction as possible. However, as cracks in the specimens had to be avoided, some angular inaccuracies were unavoidable, especially in the severely cracked high-pass samples. The test was conducted at a cross head speed of 2mm/min. Due to the size of the produced roll bonded samples, the tensile test specimens had to be scaled to the smallest extensometer available. This extensometer had an initial length of 10 mm, and could measure a maximum of 15% elongation. The pure copper and brass had a ductility of over two times this value, and the extensometer had to be reset each time it reached this strain. For the Cu and brass tests, the strain values following each reset had to be added the measured value when the test program was paused.

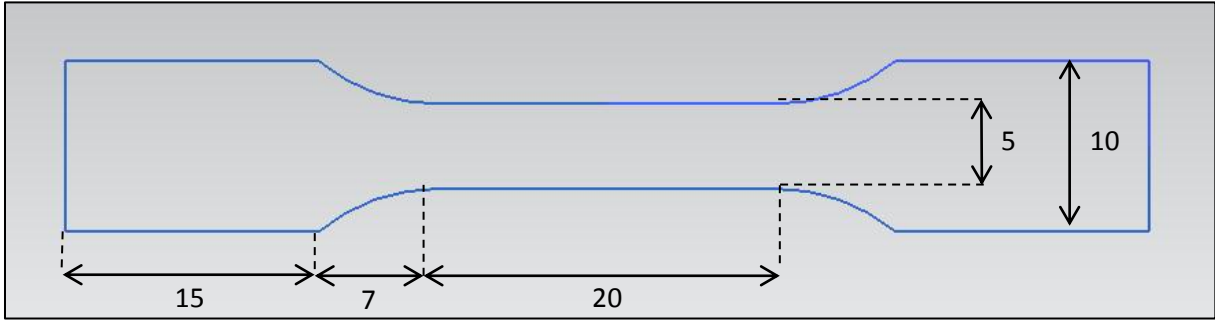


Figure 3.4: The geometry of the tensile test samples. All values are given in mm.

3.4 Three point flexural test

Samples for bend testing were cut from the 17 specimens that were cold rolled beyond the first pass. The flexural test samples measured 40 mm in length, 10.00 mm in width, and had the thickness of the rolled sheet. Precise thickness values are listed in appendix A. The samples were mounted in the same MTS 810 system as used for tensile testing, but with a flexural test set-up. Force and displacement were measured by the test system, while flexural stress was calculated from measured dimensions, test data and equation (2.6). To investigate

the delamination and/or fracture behavior of the layers in the laminate after the failure of the first layer of the sample, a relatively large total displacement was applied: 0-8mm, at a rate of 2.4 mm/min. For plotting the results in the graphs, the displacement was normalized with respect to sample thickness.

3.5 EBSD

To map the grain structure of the sample, several EBSD characterization attempts were made on a small selection of various ARB samples. The first step in surface preparation for EBSD was identical to the polishing procedure for light optical microscopy, where the sample surfaces were polished down to 0.25 micron diamond particles. The next step involved ion milling of the sample surfaces, utilizing a Hitachi IM-3000 Flat Ion Milling System, since the combination of copper and aluminum made electropolishing impossible. During the milling procedure, samples rotate while being irradiated by a stream of Ar^+ ions with energy of up to 6 keV. To achieve a mirror-like surface suitable for EBSD, a low angle between the vertical ion beam and the sample surface is required. A tilt angle of 80° from horizontal position and beam energy of 3 keV were applied to the ARB samples. The milling time was set to 45 minutes.

The samples chosen for EBSD investigation were Al/Cu 6 passes, hot rolled Al/Cu/Al 4 passes, and non-annealed Al/brass/Al 3 passes. As no data could be found on brass materials in the database of the indexing program, indexing of the brass specimen was attempted using parameters for copper.

Differences in hardness of the two metals made uniform grinding, polishing, and milling difficult, resulting in both topographical differences from layer to layer, and also different milling rates. Large strains of cold worked samples are known to impede EBSD mapping, but an investigation was attempted nevertheless.

4 Experimental results

4.1 ARB specimens

When rolled for more than 4 passes, both the brass configurations lead to severe cracking of the specimens. The cold rolled Al/Cu/Al sample was cracked in a similar manner after the 5th pass, but parts of the sheet were intact, and possible to include in further analysis and characterization. The cracks seemed to persistently initiate along the sides of the specimens, in close proximity to the aluminum rivets used for pinning the ends of the material. Furthermore, the cracks propagated in a curved manner towards the rolling direction and the center of the sheet. This resulted in split specimens where each half bent outwards from the center, in transverse directions.

4.2 Light optical micrographs

The micrographs obtained from the optical microscopy of the hot rolled copper specimens at 50x magnification are displayed in figure 4.1.

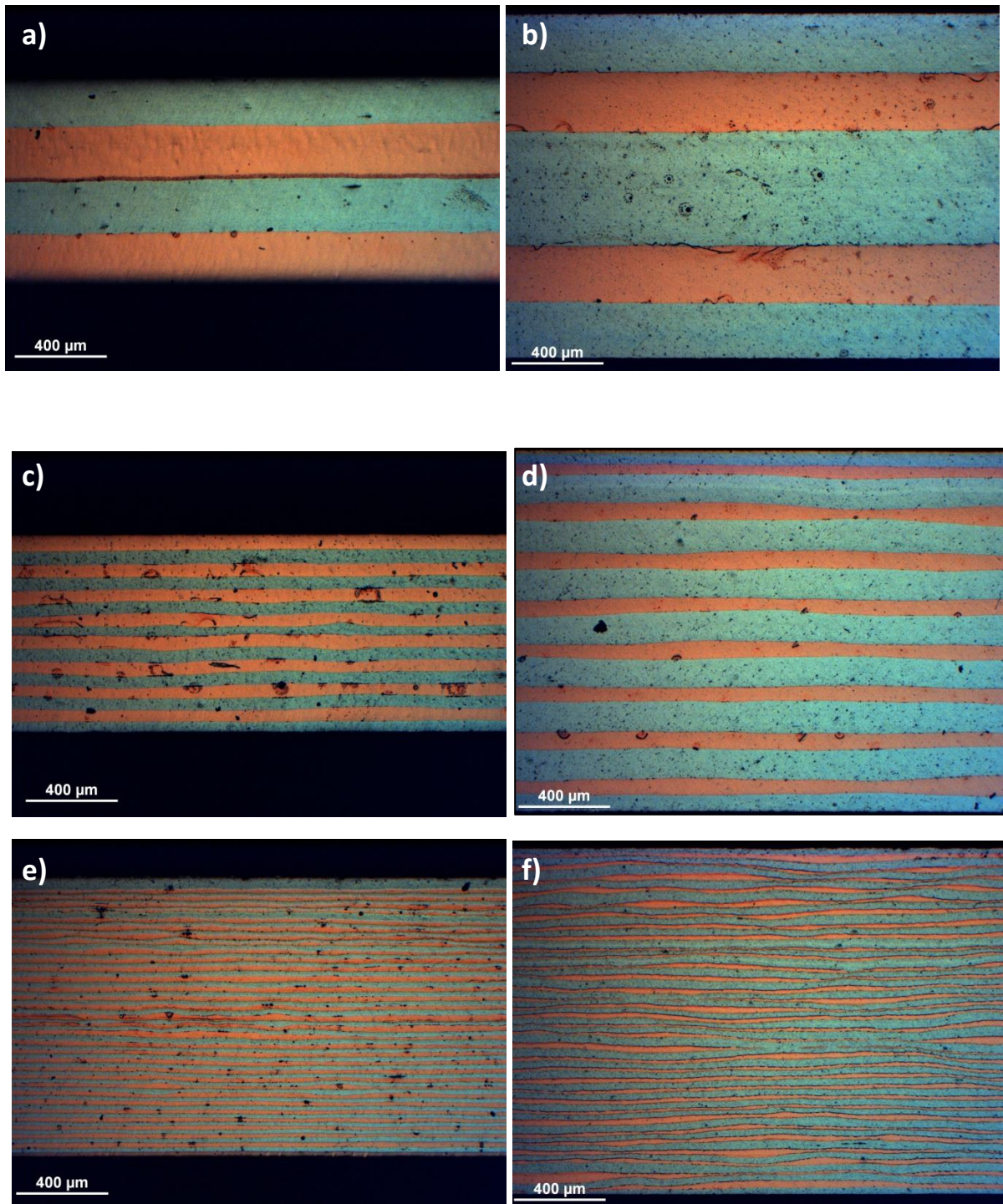


Figure 4.1: Optical micrographs taken at 50 times magnification. Picture a), c) and e) show the Al/Cu sample at 2, 4, and 6 passes, respectively. Picture b), d) and f) show the hot rolled Al/Cu/Al sample at 2, 4 and 6 passes, respectively.

The hot rolled Al/Cu/Al sample shows an extensive amount of necking, and several points of fracture, in the copper layers after six passes. Some signs of necking can be seen in the Al/Cu

sample after an equal amount of passes, but no fracture is observed, and the overall layer distribution is smoother and straighter compared to the other parallel.

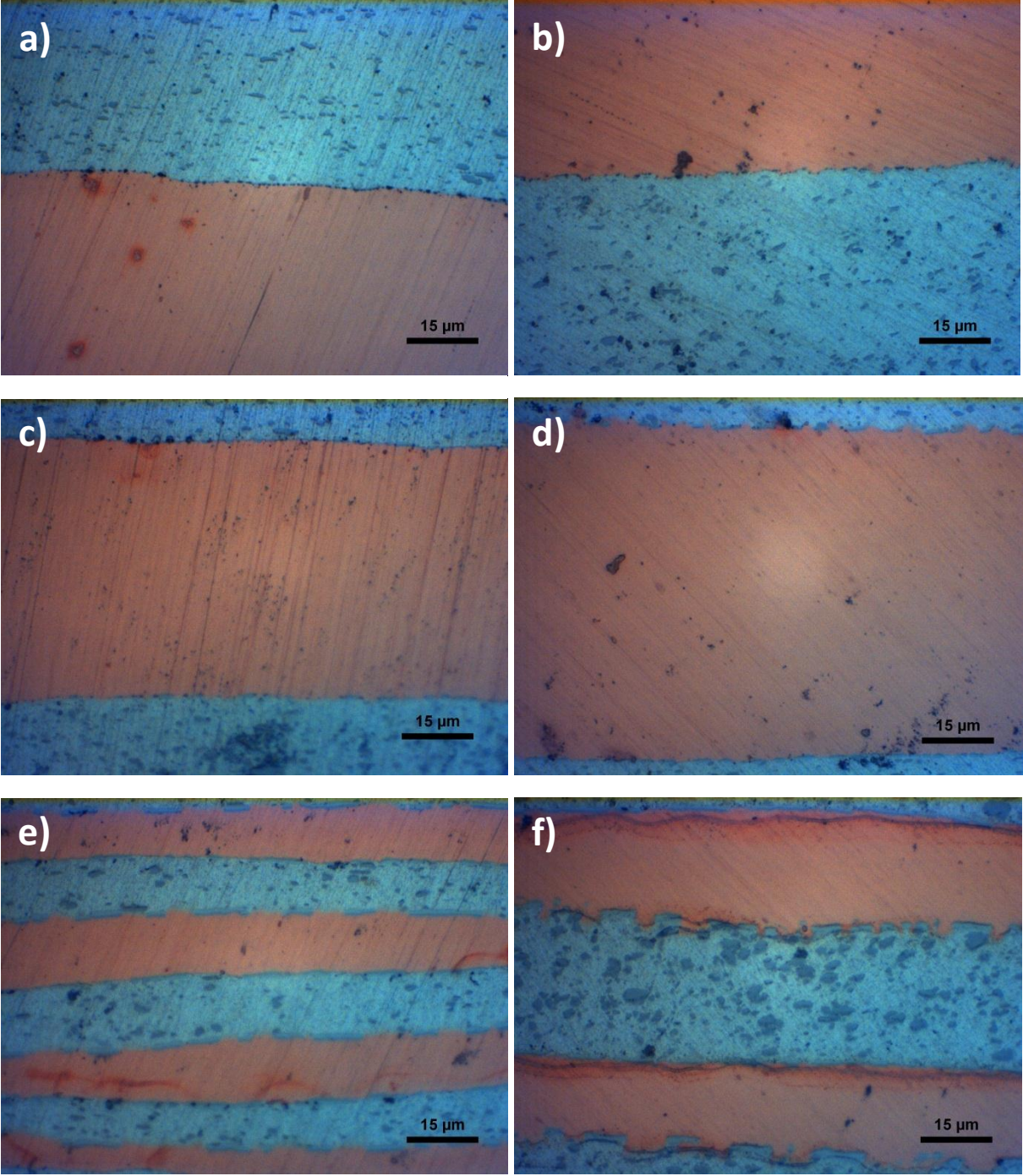


Figure 4.2: Optical micrographs taken at 1000 times magnification. Picture a), c) and e) show the Al/Cu sample at 2, 4, and 6 passes, respectively. Picture b), d) and f) show the Al/Cu/Al sample at 2, 4 and 6 passes, respectively.

At 1000x magnification the interfaces in the 6 pass samples, along with the 4 pass hot rolled Al/Cu/Al sample, look serrated and deformed in the normal direction of the composite. The other samples have smoother interfaces with black spots spread out along the interface, and the cross-deformation is less prominent.

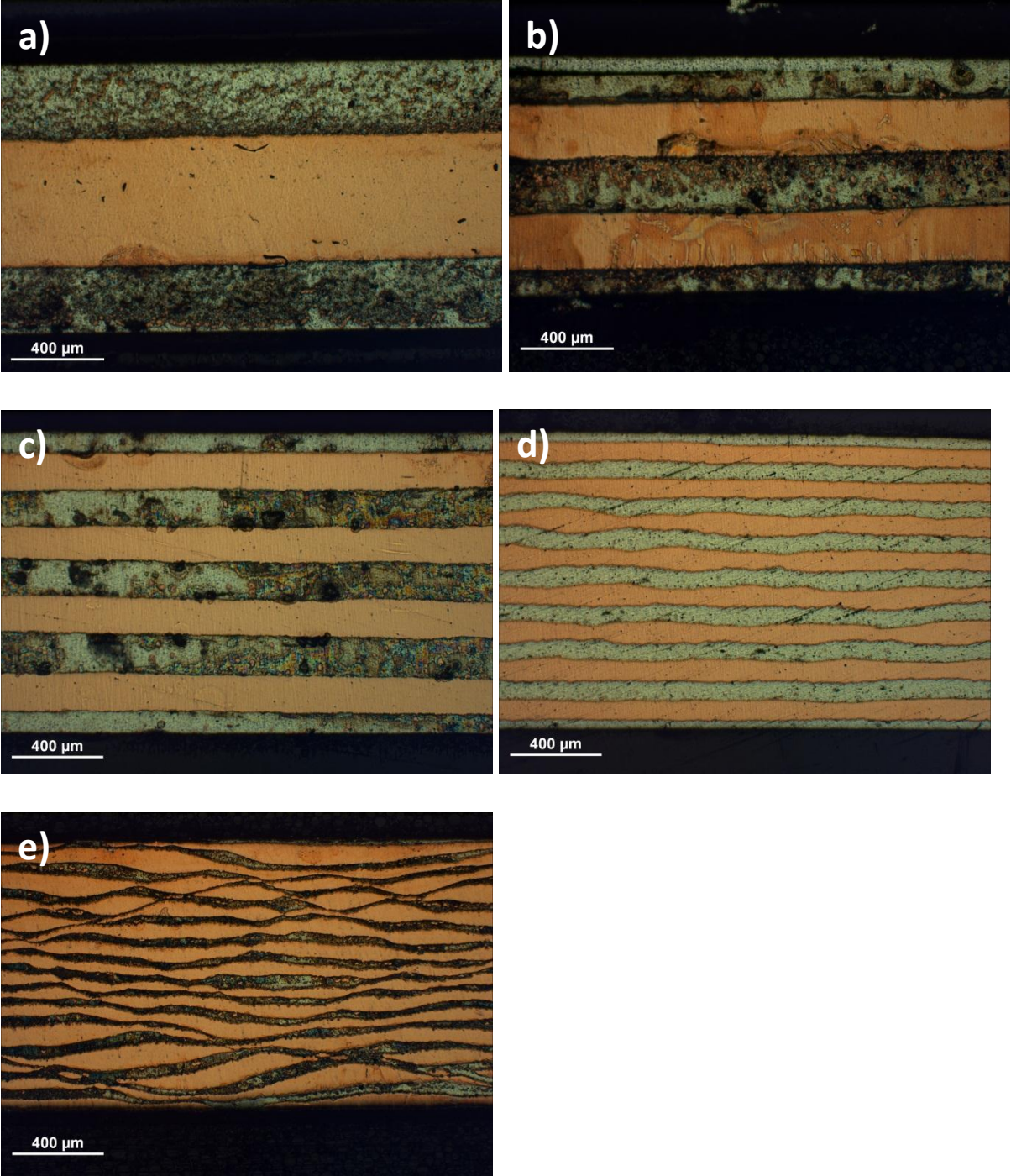


Figure 4.3: Micrographs of the CARB Al/Cu/Al specimens at 50X magnification. Pictures a), b), c), d) and e) show the material at 1, 2, 3, 4 and 5 passes, respectively.

The layer structures of the CARB Al/Cu/Al specimens are depicted in figure 4.3. For the first 3 passes, no apparent difference this and the hot rolled specimens is observed. However, after 5 passes of roll bonding, the copper layers show extensive necking behavior and undulating lines that seem to propagate across layers in a wavelike pattern.

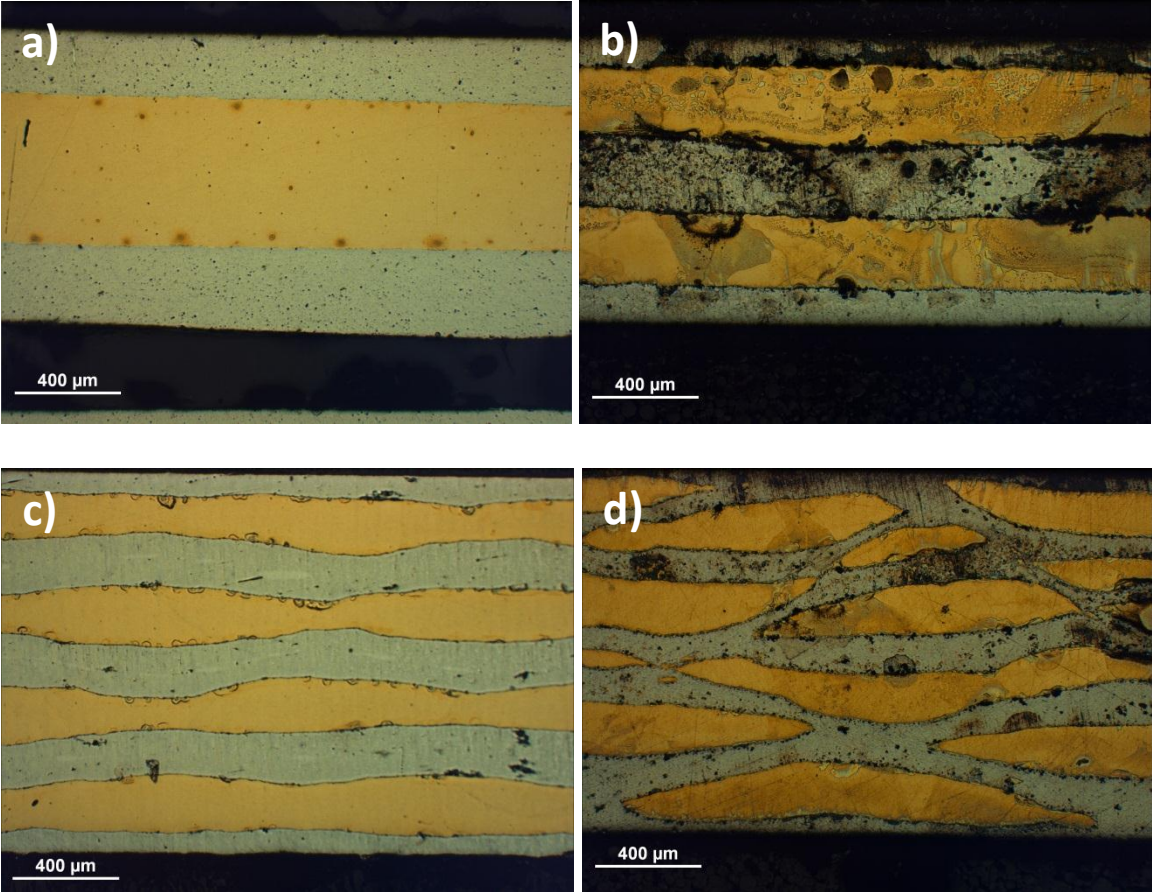


Figure 4.4: The four laminates made from non-annealed sheets of brass, in ascending order with respect to the number of passes. Pictures taken at 50X magnification.

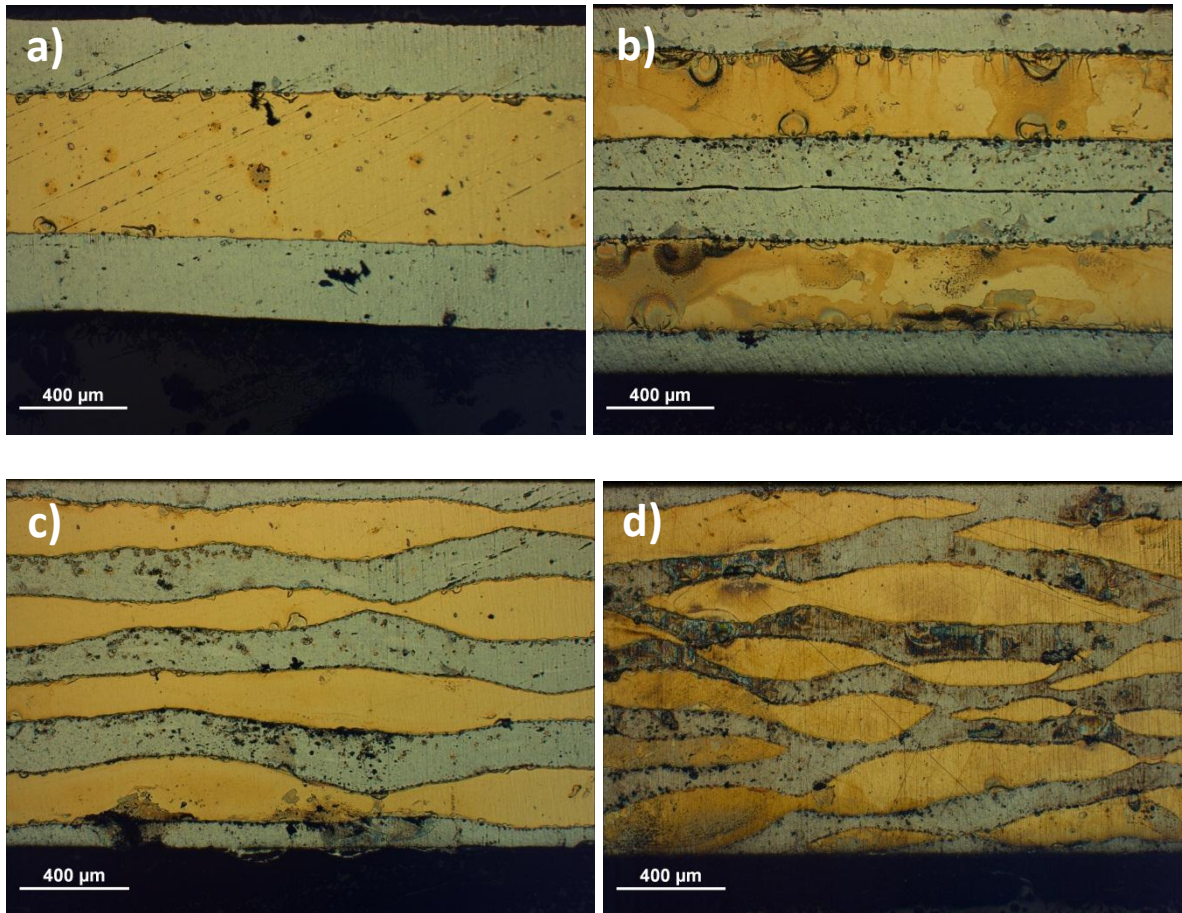


Figure 4.5: Micrographs of the CARB Al/brass/Al parallel with initially annealed brass, at 1, 2, 3 and 4 passes, respectively. 50X magnification.

Only small differences separate the two brass groups, as necking occurs in both parallels at 3 passes, fracture after 4 passes, and neither of them made it through the 5th pass. When comparing fig. 4.4 d) and 4.5 d), the annealed brass seems more continuous than the non-annealed brass layers, as not all of the necks have resulted in fracture yet. However, in fig. 4.4 c) and 4.5 c), it may seem as necking occurs at an earlier stage in the initially annealed brass. The black, horizontal line in the middle of fig. 4.5 b) is a crack between two aluminum layers.

4.3 Tensile test results

The engineering stress vs. strain results, from the tensile tests of the materials rolled at 350°C, are plotted in the following 3 figures. The evolution of strength and ductility with increasing number of passes is shown for both the Al/Cu and Al/Cu/Al type of samples. The third figure compares results for the hot rolled 6 pass samples of Al/Cu and Al/Cu/Al.

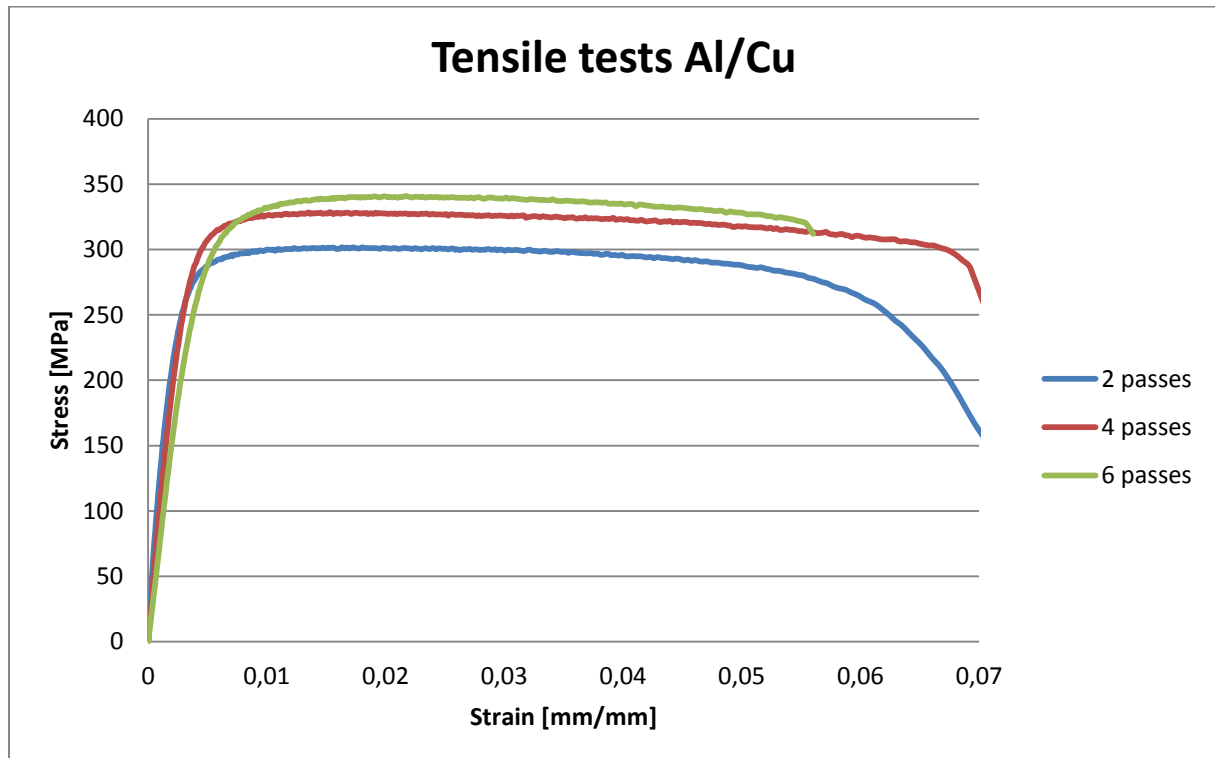


Figure 4.6: Tensile test results for the Al/Cu parallel of samples rolled at 350 °C.

The strength of the material is increased with increasing number of passes. After 2 passes, the ultimate strength is 300 MPa. This is raised to 335 MPa after 4 passes and to 340 MPa after 6 passes.

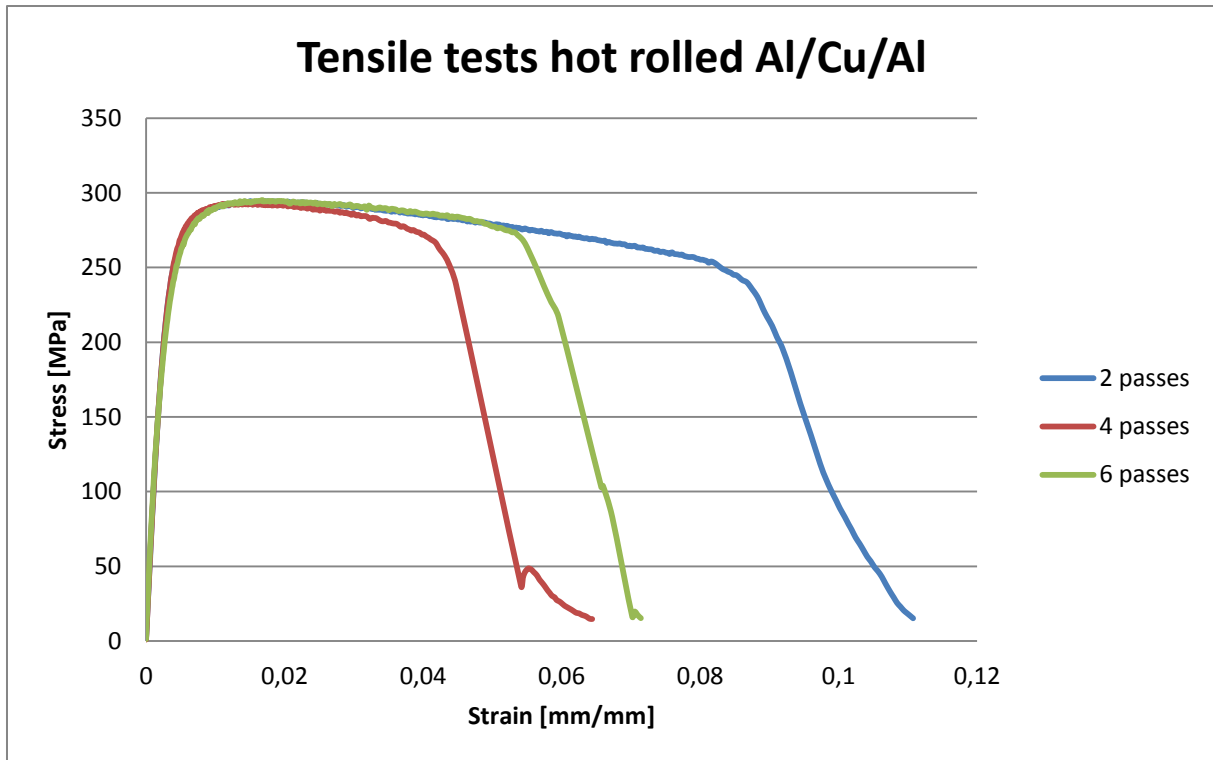


Figure 4.7: Tensile test results for the Al/Cu/Al parallel of samples rolled at 350 °C.

For the Al/Cu/Al, the ultimate strength remains virtually unchanged after each pass, staying at a constant 295 MPa. The yield strength is approximately constant as well. The results may indicate a decrease in ductility from 2 to 4 passes and an increase from 4 to 6 passes.

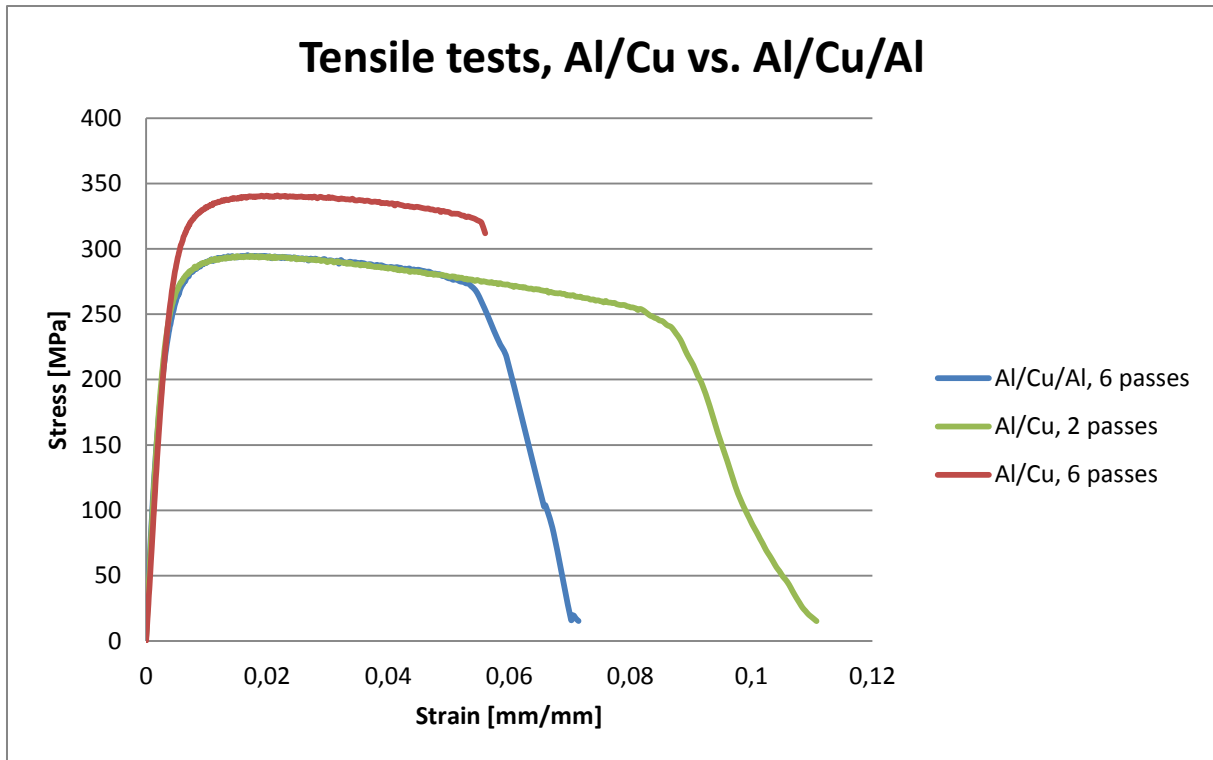


Figure 4.8: Comparison of the tensile test results of the 6 and 2 pass Al/Cu and 6 pass Al/Cu/Al samples (Rolled at 350 °C).

The plots in figure 4.8 show that after 6 passes, the strength of the Al/Cu sample has increased to a greater extent than the Al/Cu/Al sample, while being able to withstand approximately the same amount of deformation before fracture occurs.

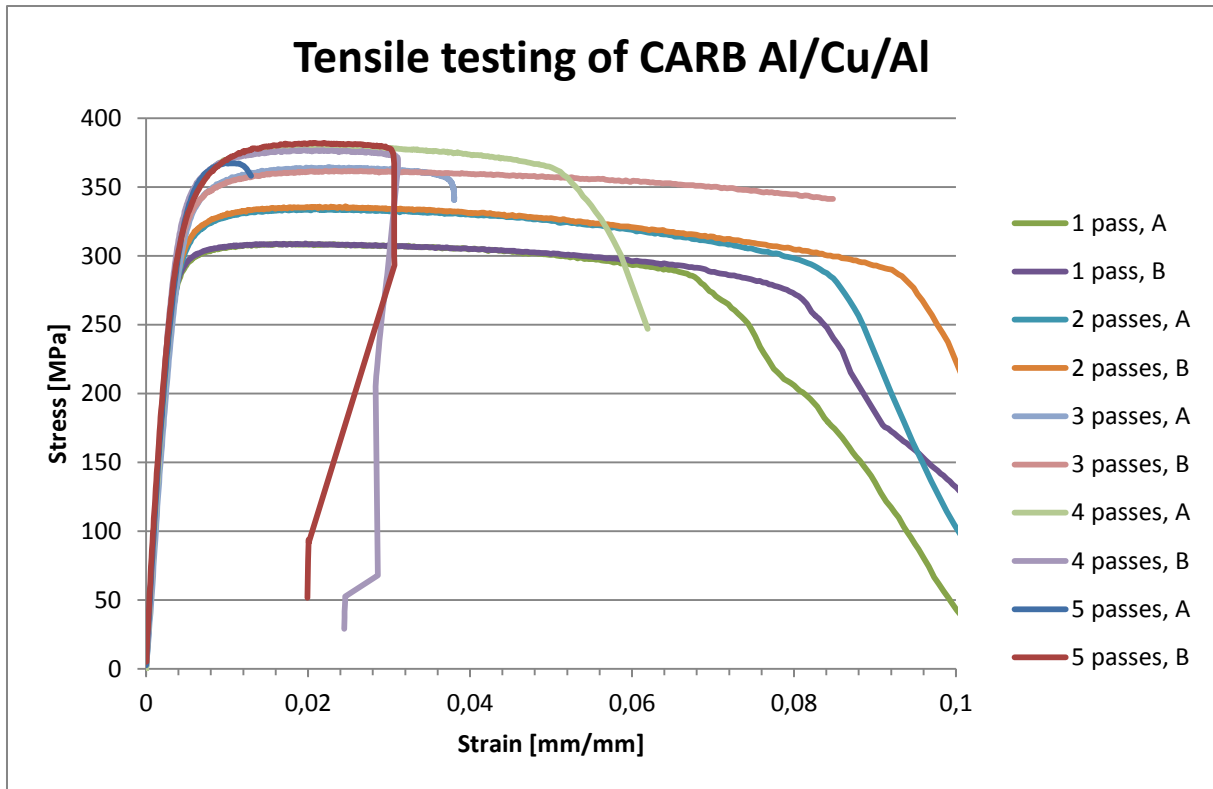


Figure 4.9: Tensile test results for the CARB Al/Cu/Al samples. Two parallel samples were tested for each number of passes.

For the cold rolled Al/Cu/Al sample, the increasing amount of accumulated cold working is evident. With each pass of rolling, the tensile strength increases, except between the 4th and 5th passes. The ultimate tensile strengths are: 308 MPa for 1 pass, 335 MPa for the 2nd pass, 360 MPa after 3 passes, 376 MPa for the 4th pass, 367 MPa for sample A at 5 passes, and 381 MPa for 5 passes B. The fracture elongation seems to increase from ca. 7% after the first pass to between 8 and 9% after the second pass of ARB. At a higher number of passes, the ductility of the materials seems less consistent. For 3 passes, sample A yields approximately 3.7% strain before rupturing, while sample B could be deformed over 8%. For the 4 pass specimens, the value range from 3 to 5%, while the 5 pass samples result in 1 and 3% elongation for sample A and B respectively.

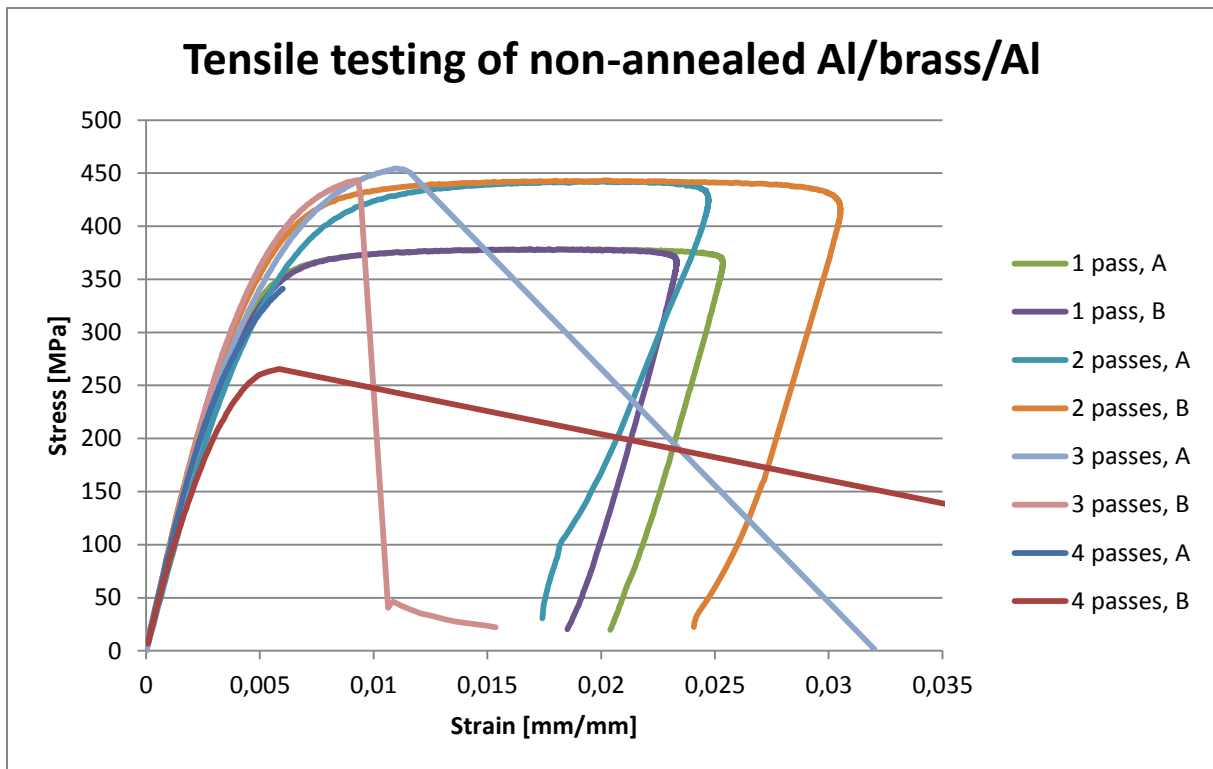


Figure 4.10: Tensile test results for non-annealed Al/brass/Al sheets. Two samples were tested for each number of passes.

After the first pass of roll bonding, the specimens made from non-annealed sheets of brass exhibit an ultimate tensile strength of 378 MPa, and can withstand between 2 and 2.5% elongation. The 2nd pass samples maxed out at 442 MPa, and between 2.45 and 3% elongation upon rupturing. The strength continued to increase to 3 passes, although not giving coinciding results for those samples. Specimen A had a strength of 454 MPa, while specimen B lasted until reaching a stress of 441 MPa. The ductility of these samples were 1% for A and 0.88% for B. For the last pair of samples, the fracture elongation was relatively equal, ending up at around 0.56% for both tests. The 4 pass specimens showed signs of brittle behavior and varied greatly: Between 264 and 335 MPa.

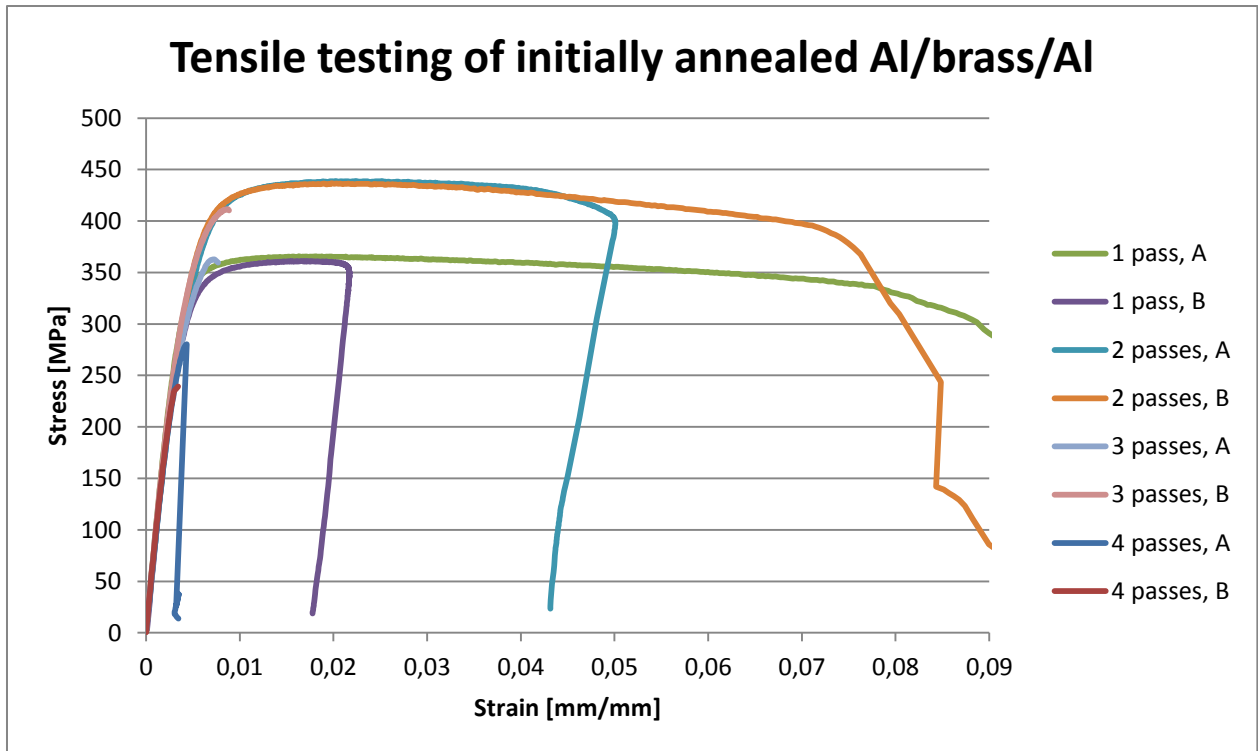


Figure 4.11: Tensile test results for the parallel of brass specimens with initially annealed brass. Two parallels from each number of passes were tested.

1st pass samples A and B had similar tensile strength, at about 360 MPa. Sample B fractured at ~2% elongation, and sample A had about 9% elongation when fracturing. After 2 passes of ARB, the material achieved the highest strength among all the parallels: 437 MPa. One sample fractured at 5% strain, while the other lasted until ca 7.5% deformation. The 3 pass samples both fractured at about 1% deformation. At that point, sample A had reached 362 MPa stress, and sample B experienced stress at a magnitude of 411 MPa. Failure of both 4 pass samples happened at ~0.35% strain. The tensile strengths were 280 MPa for sample A and 239 MPa for sample B.

For the brass materials, the results indicate a trend of more homogenous fracture elongation with increasing number of passes, while the uncertainty associated with the ultimate tensile strength increases as more cycles of ARB are applied.

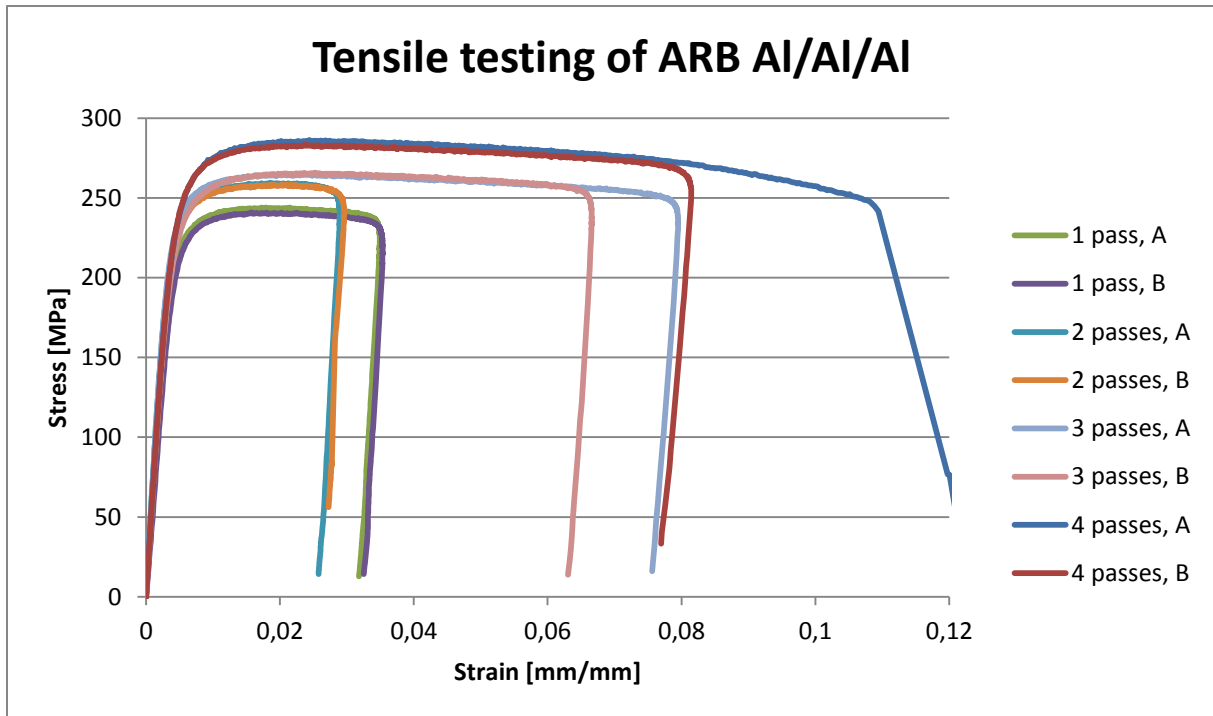


Figure 4.12: Tensile test results of the CARB Al/Al/Al sheets. Two parallels from each material were tested.

The tensile strengths of the Al/Al/Al laminates were found to be 242 MPa, 257 MPa, 265 MPa, and 285 MPa for 1, 2, 3, and 4 passes, respectively. Note that beyond the 2nd pass, both the strength and the ductility of the materials increase with increasing amount of cold working. The variation in ductility apparently increases as well.

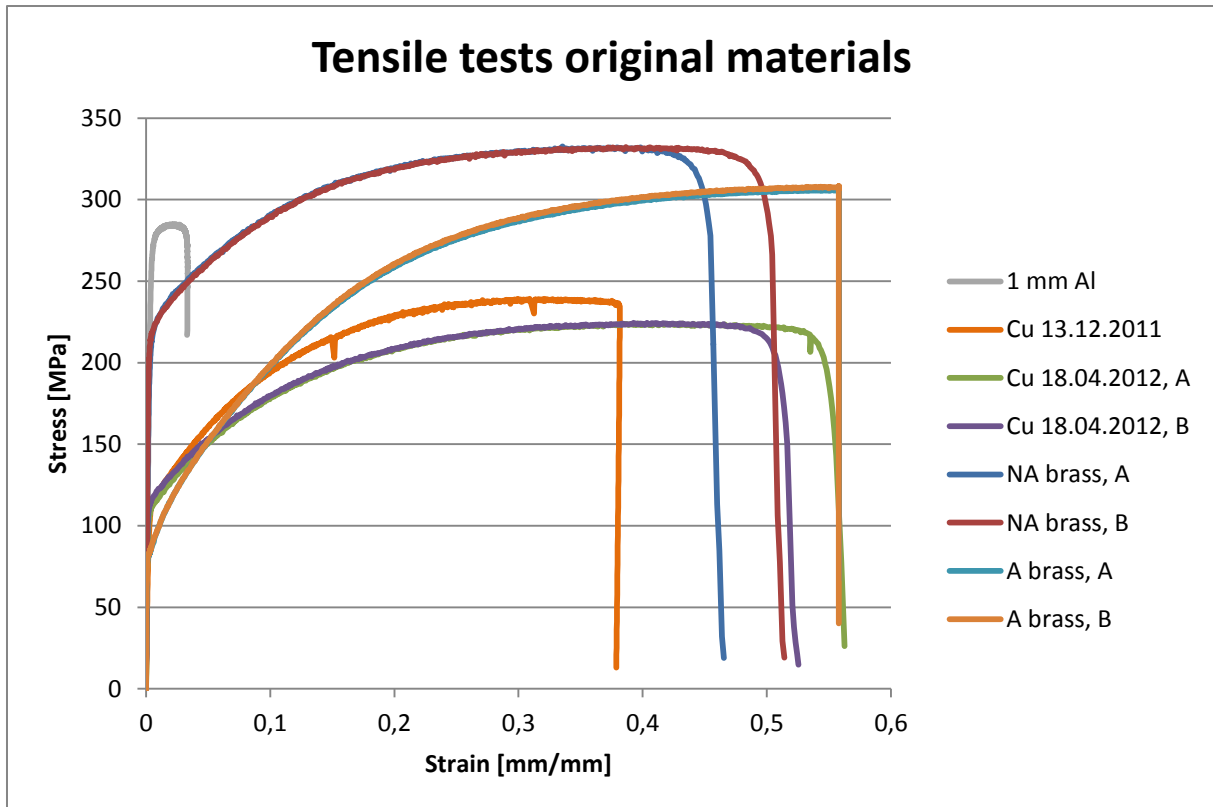


Figure 4.13: Tensile test results for the original materials used in creating the preforms.

The aluminum sheets used in the preforms had been cold rolled from a thickness of 20 mm to a thickness of 1 mm, without further treatment. This amount of cold working is consistent with the increased strength, low work hardening, and low elongation shown in the tensile test results. The 0.5 mm sheets used in creating the hot rolled preforms were deformed to such an extent that they were uneven, and were thus not suited for machining of tensile samples. Nevertheless, these sheets can be assumed to be in the same range as the 1 mm sheets, with stress-strain behavior shifted slightly up and to the left when compared to the results for the 1 mm Al sheet in fig. 4.13. The measured tensile strength of aluminum was ~282 MPa, and fracture occurred before reaching 3.5% strain.

The commercially pure copper had an ultimate tensile strength of 238 MPa, when tested in December, and elongated extensively, to approximately 38%, before fracturing. After 4 more months of storage at room temperature, the strength had been lowered to 224 MPa, but the material extended to between 50 and 55% strain before breaking.

The non-annealed brass was the strongest of the component materials, at 332 MPa, with an elongation of 45-48%. When annealed at 600°C for one hour, the ultimate strength dropped to 307 MPa, while a ductility of almost 60% was achieved.

The downward spikes in the tensile test curve for Cu and brass mark the points where the extensometer was recalibrated. The annealed brass specimens, however, extended far more than expected, and the vertical lines at the end of the graph mark the maximal limit of the extensometer. Although accurate values were not obtained, those samples fractured in the 57-59% elongation range.

Table 4.1: Comparison of maximum tensile strength achieved for each parallel of samples

	Number of passes	Max strength achieved	Remarks
Hot rolled Al/Cu	6	340 MPa	
Hot rolled Al/Cu/Al	All	295 MPa	
CARB Al/Cu/Al	5	381 MPa	Significant variation between parallel samples
CARB non-annealed Al/Br/Al	3	454 MPa	Results for specimen A, as specimen B showed 13 Mpa lower tensile strength
CARB Al/Br/Al, initially annealed brass	2	437 MPa	
Al/Al/Al	4	285 MPa	

4.4 Three point flexural test results

One flexural test specimen was taken from each cold roll bonded specimen and tested at 0-8 mm deflection. As the thickness of the rolled sheets exhibited large variations, the deflection was divided by sample thickness as a way of normalizing the deflection value. The measured thickness values are given in table A.2. Calculated flexural stresses from equation 2.6 are, in the following figures, plotted against deflection divided by sample thickness.

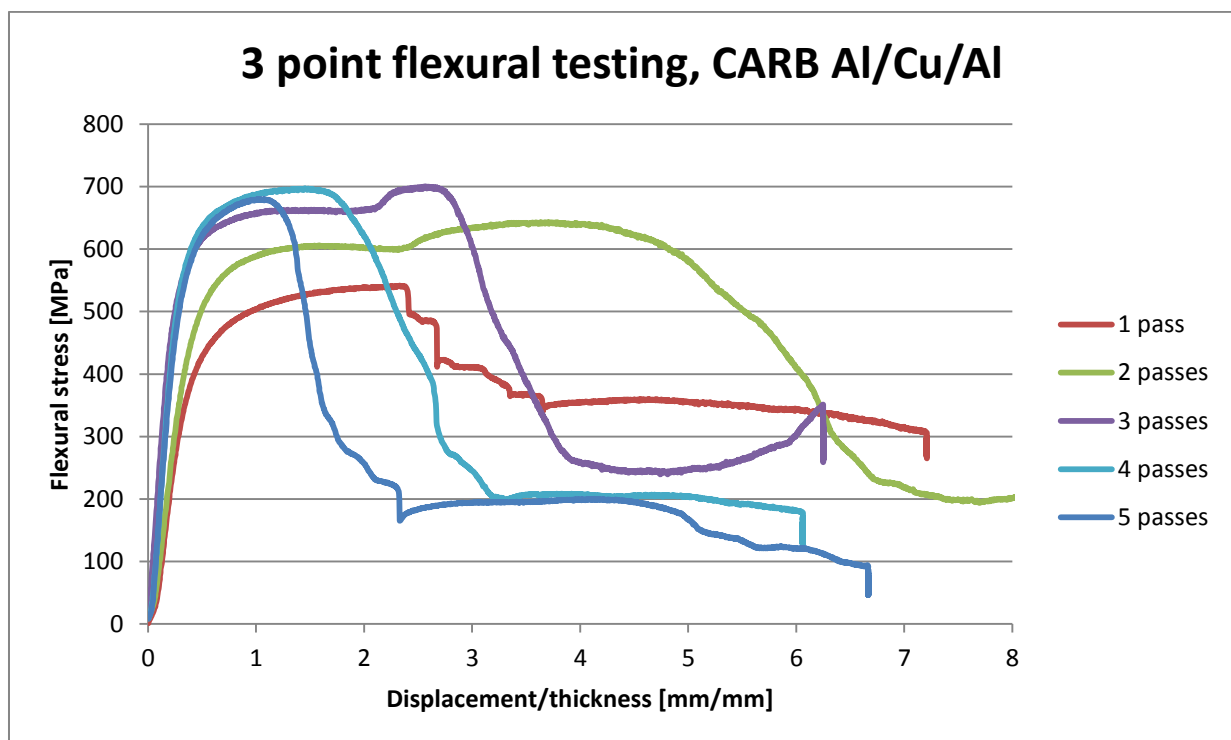


Figure 4.14: Flexural test results for the CARB Al/Cu/Al specimens.

The first of the CARB Al/Cu/Al samples exhibited a flexural strength of 541 MPa, and the first layer in the sheet fractured at 2.4 displacement. Beyond that point, the graph shows several sudden dips in stress, as layers delaminate and/or rupture. The last four displacement units of the test, the graph stays smooth. As expected, the 2 pass sample is stronger, and reaches a temporary maximum at 605 MPa stress and 1.3 deflection. Upon reaching 2.2 deflection, the applied stress begins to increase again, reaching a global maximum of 641

MPa at 3.5 before smoothly declining. The highest flexural strength for the copper samples was achieved by the 3 and 4 pass samples. Both of them reached practically the same stress, with the 3 pass sample at 698 MPa and the 4 pass sample at 697 MPa. The 4 pass sample peaked at 1.9 deflection, while the 3 pass sample's limit was at 2.4. The 5th sample yielded weaker results, with 675 MPa max strength at 0.9 deflection.

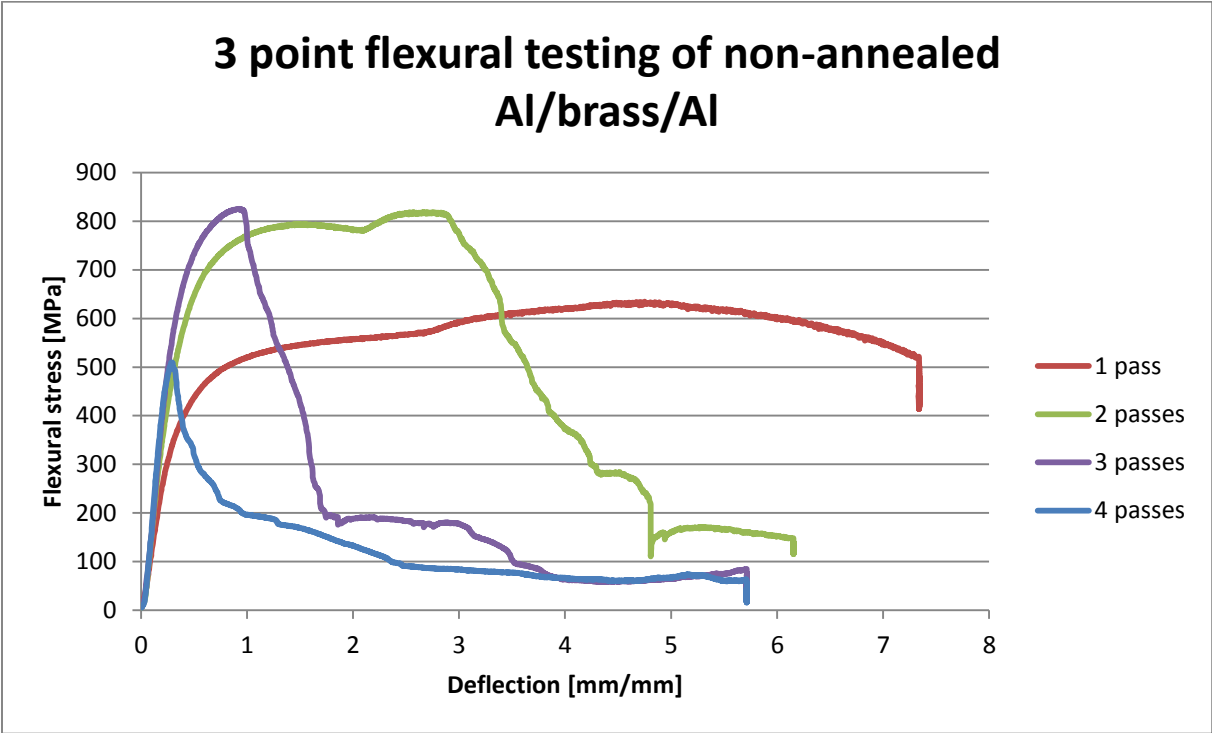


Figure 4.15: Flexural test results for the non-annealed parallel of Al/brass/Al specimens.

The 1 pass sample was deformed deflectionwise smoothly, with a flexural strength of 634 MPa peaking at 4.7 deflection. The 2 and 3 pass samples showed comparable strengths, with 819 MPa at 2.7 and 821 MPa at 0.9, respectively. Like the 2 pass sample from the Al/Cu/Al tests, the 2nd NA Al/brass/Al sample reached a local maximum of 793 MPa stress at 1.5 displacement, before additional strengthening started at 2.0. The 4 pass sample exhibited a significant decrease in strength, with 509 MPa peak stress when bent to 0.3 normalized deflection.

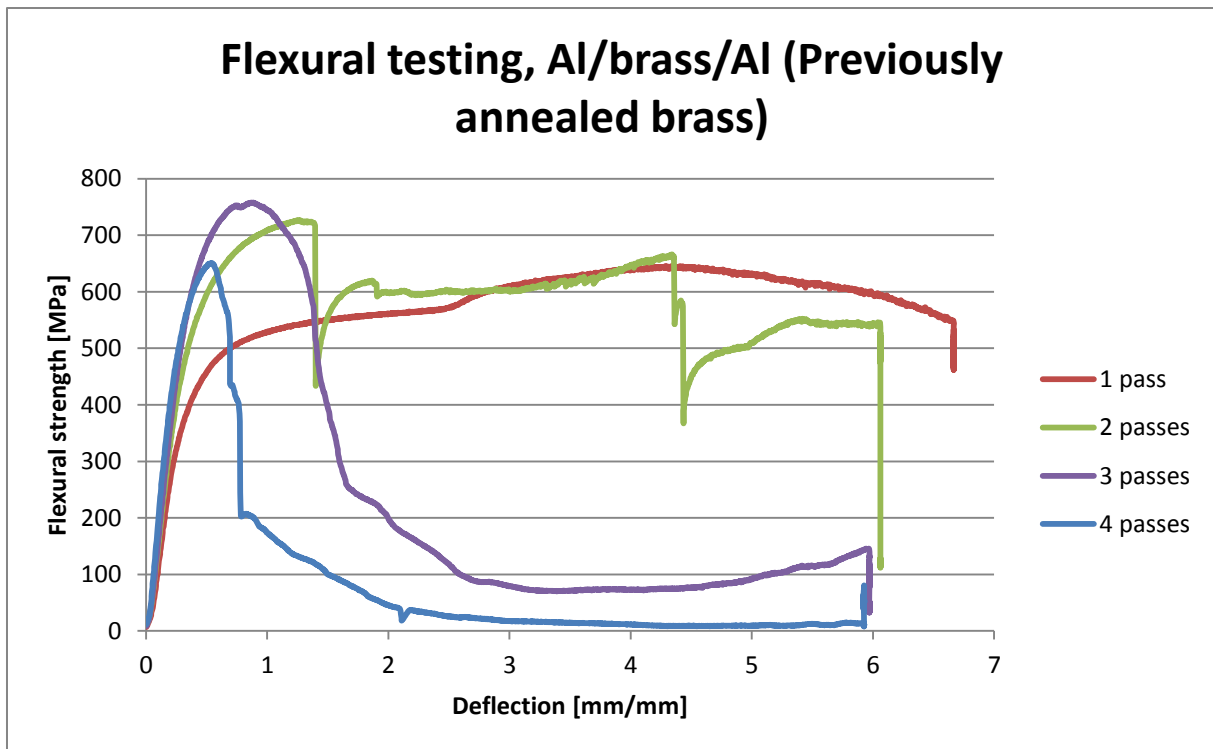


Figure 4.16: Flexural test results for the annealed parallel of Al/brass/Al specimens.

The flexural strength of the 1 pass sample was measured to be 643 MPa at 4.4 deflection. At 2.5 deformation, a sudden increase in stress is observed. The 2 pass sample experienced maximum stress after 1.2 mm, showing a flexural strength of 723 MPa. The strength of the 3 pass sample was even higher, with 758 MPa at 0.9, while the 4 pass sample was at approximately the same strength level as the 1 pass sample, with 648 MPa strength at 0.5 deflection.

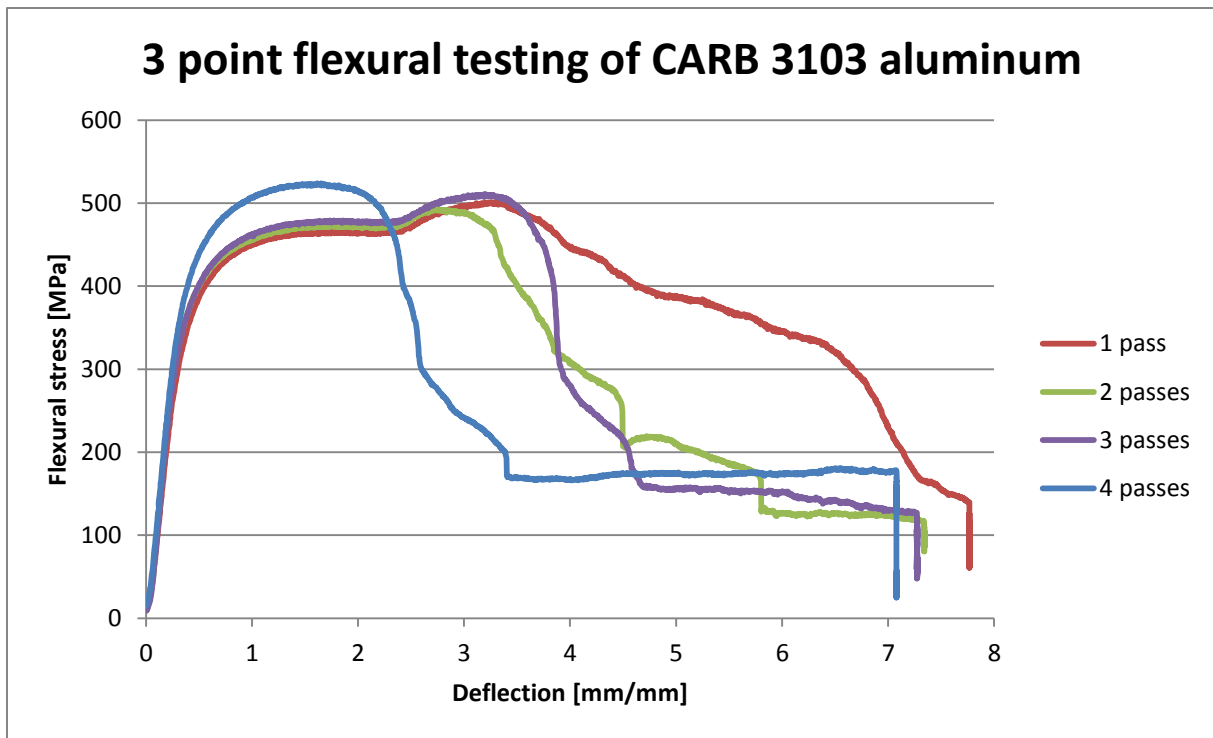


Figure 4.17: Flexural test results for the Al/Al/Al specimens.

For the three first passes of ARB of the aluminum preforms, the bend test results were within close range of each other. The 1 pass sample had strength of 500 MPa at 3.2 deflection, the 2 pass sample possessed strength of 490 MPa at 2.8, and the 3 pass specimen was subject to maximum stress of 510 MPa at 3.2. All the specimens had a sudden stress increase in the 2.4-2.5 range. The 4th specimen separated itself from the other specimens, giving a maximum stress of 524 MPa at 1.6.

All of the bend bimetal test specimens fractured at the outermost layer, while none of the inner half of layers were deformed until failure.

Table 4.2: Comparison of maximum flexural strength achieved by each parallel of samples.

	Number of passes	Max strength achieved	Remarks
CARB Al/Cu/Al	3	698 MPa	4 pass sample only 1 MPa lower strength
CARB non-annealed Al/Br/Al	3	821 MPa	2 pass sample only 2 Mpa lower strength
CARB Al/Br/Al, initially annealed brass	3	758 MPa	
Al/Al/Al	4	524 MPa	

4.5 EBSD results

Polishing the metal laminates for EBSD proved to be a challenge, as the softer Al layers were worn down at a higher rate than the hard copper or brass layers. When the copper parts of the material were milled to a satisfactory extent, the aluminum surfaces were pitted and deformed when viewed in imaging mode in the SEM.

This is demonstrated in figure 4.18, as the difference between the results for the copper and the aluminum layers in hot rolled Al/Cu/Al of 4 passes vary significantly. In part a) and c), no deformation of the grains in the horizontal rolling direction is observed, and most of the indexed area contains just single pixels of multiple colors. As a consequence of this, one can assume that the results are incorrectly indexed.

Fig. 4.18 b) and d) display grains of shape and orientation of a nature that can be expected after rolling. The orientation difference between grains along the rolling direction is lower than in the normal direction of the material. From the center of image d) and diagonally upwards to the right, a shear band can be observed. This formation of shear bands is an instability mechanism that may affect layer continuity in addition to necking due to strain.

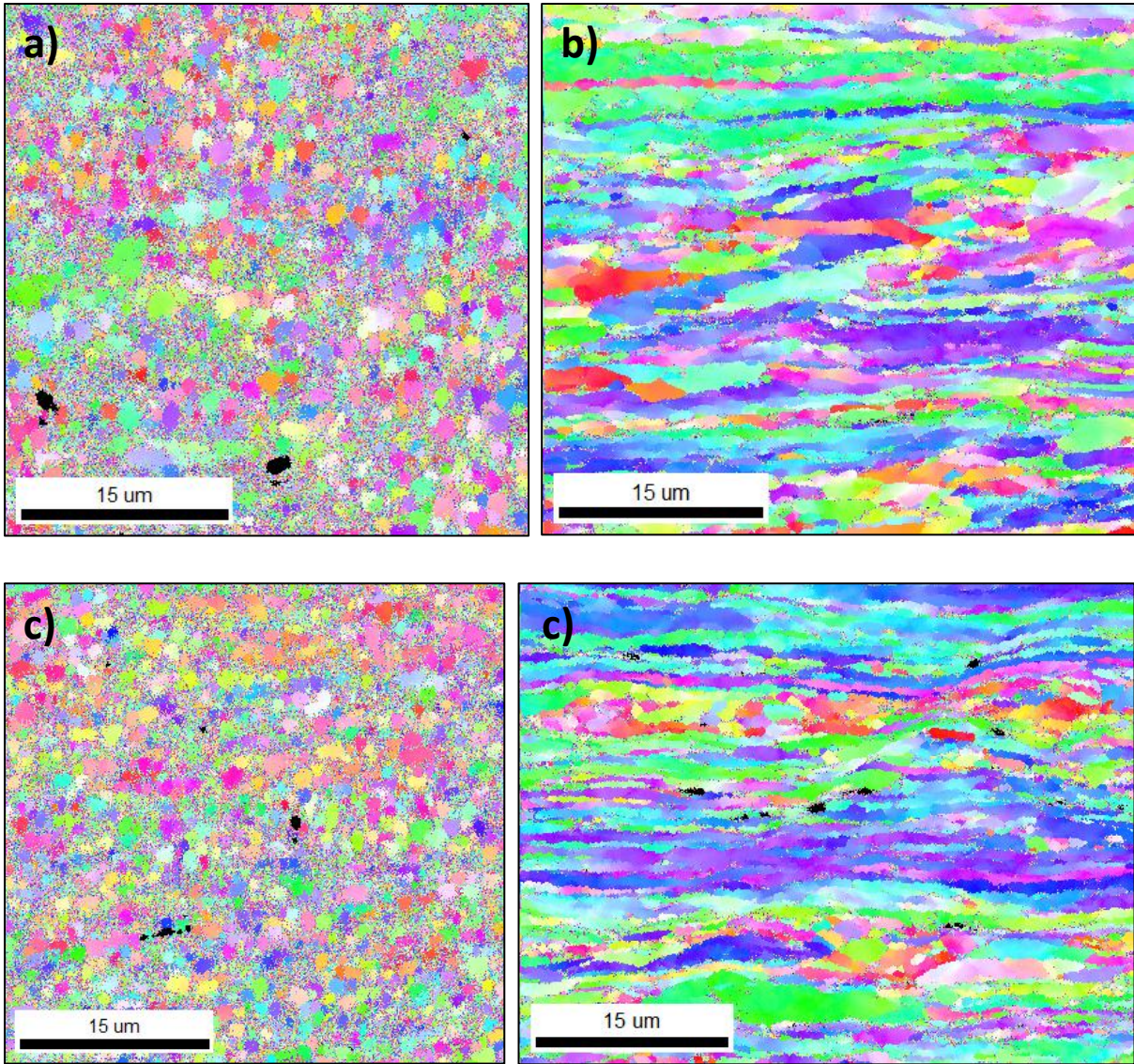


Figure 4.18: EBSD mapping results for the hot rolled Al/Cu/Al specimen of 4 passes of ARB. Picture a) and c) show the results for aluminum layers, in positions close to the surface and close to the center of the specimen, respectively. Picture b) displays results for a copper layer close to the surface, and the mapping in picture d) is done close to the center of the sample. 1500X magnification.

EBSD results for the Al/Cu 6 pass sample are shown in fig. 4.19. The grains are elongated in the rolling direction, and are of an overall relatively uniform orientation.

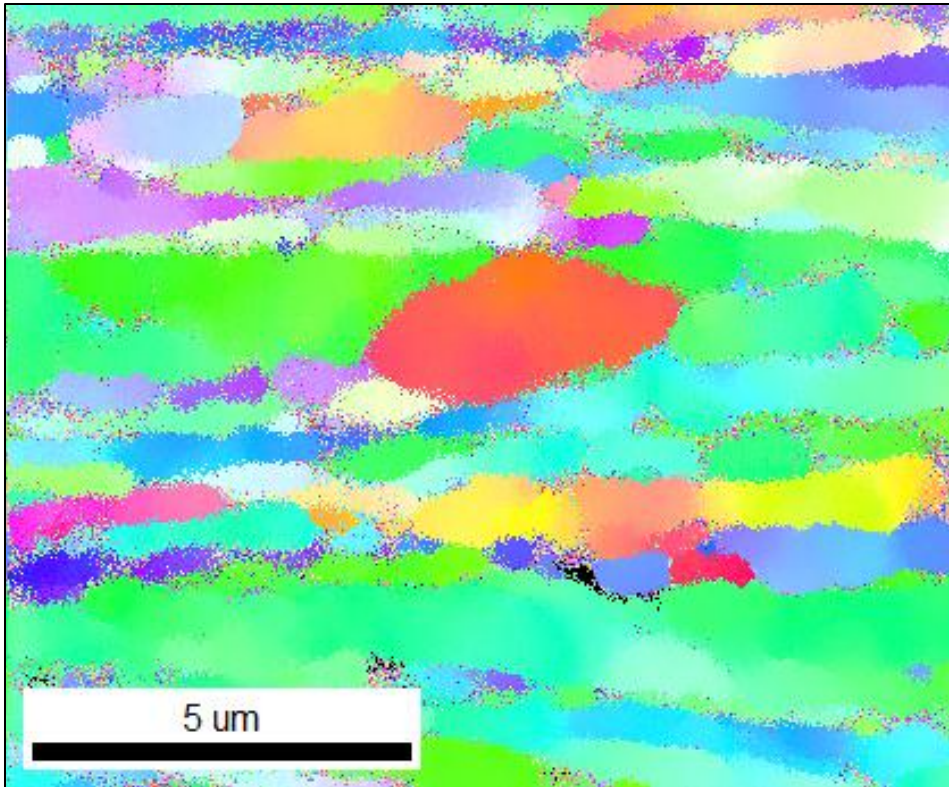


Figure 4.19: EBSD imaging result for Al/Cu 6 passes. 6000X magnification

The non-annealed Al/brass/Al 3 pass specimen did not yield any EBSD results. The same milling parameters as for the other samples were used. As a result, the aluminum layers were not indexable. In addition, the indexing database did not contain any information on mapping of brass materials. Using copper parameters did not yield viable results.

5 Discussion

5.1 Micrographs

In the hot rolled 6 pass samples, the copper layers in the Al/Cu sample did not neck or fracture to the same extent as the copper layers in the Al/Cu/Al sample. As all the other parameters were identical in each case, this phenomenon is necessarily related to the thickness ratio H (equation 2.1) of the hard copper layer to the total initial thickness of the sample. The H -ratio was 0.5 for Al/Cu and $1/3$ for Al/Cu/Al. These results are consistent with the relations given in equation 2.1 and 2.2.

At a higher amount of passes, the interfaces have jagged edges, where the material has been deformed parallel to the normal direction. This could be caused by extrusion between fragments of the oxide layers, different flow characteristics, and/or residual deformation from surface preparation (brushing).

When comparing the cold rolled Al/Cu/Al specimens to the hot rolled parallel, the layer structure is approximately the same for the first four passes of ARB. After the 5th pass, however, the cold rolled material was necked and fractured to a greater extent than the hot rolled specimens were after 6 passes. This is an indication of greater amount of equivalent cold working strain in the cold rolled sheets, leading to earlier failure of the harder metal. Wave-like patterns across the deformed layers can be observed. These undulations could be caused by shear banding in a deformed copper layer propagating across layers in the normal direction, or they could be a product of the flow traits of the bimetallic system.

At 3 passes of ARB, both types of brass specimens show signs of incipient necking. The annealed brass layers are slightly more necked than their non-annealed counterpart. One probable cause for this development is that between initial bonding of the different materials during the first pass and the subsequent two passes, the total work hardening could be greater

for the previously annealed brass than the non-annealed layers. This would lead to higher shear stresses at the interfaces and more rapid necking of the brass layers. Both 4 pass samples have discontinuous, ruptured brass layers. The annealed specimen has retained more necks than the non-annealed brass. Despite necking at an earlier stage, it seems that the more ductile, annealed layers are more capable of sustaining layer continuity than the sheets that were not annealed. These differences are, for ARB purposes, insignificant beyond the 4th pass, as none of the materials could withstand the deformation of another pass of roll bonding.

5.2 Tensile tests

For hot rolled Al/Cu/Al, the strength of the material remained constant with varying number of passes, while for the Al/Cu samples, the strength increased with each cycle of ARB. As the materials were identically treated, the variations must be a consequence of the stacking difference. For the Al/Cu/Al configuration, aluminum is the only metal that is in contact with the rolls, while in Al/Cu, one copper layer is in contact with the rolls during each pass. Since the rolls are at room temperature, and copper conducts heat better than aluminum, this could cause more rapid cooling of the Al/Cu specimen, and a slightly higher amount of cold deformation. The steady state flow stress may be dependent on temperature in addition to strain rate.

The two tempers of brass materials gained significant strength, in the 75 MPa range, from the 1st to the 2nd pass. The non-annealed sheets showed an additional strength gain after 3 passes, whereas the annealed sample failed at lower stresses than the 2 pass samples. This is probably a result of the faster necking/instability formation of the annealed brass, as observed in the micrographs. The necked brass layers fracture at lower tensile stresses in the previously annealed material than the more uniform non-annealed brass layers. The tensile strengths of the 4 pass samples are severely reduced, as the brass layers are no longer continuous, and the Al matrix has to keep the sheet together.

As expected, the strength in the Al/Al/Al laminate increased with each pass of ARB. The accumulated cold working strengthens the material, and would presumably lead to diminished

ductility as well. As fig. 4.12 clearly illustrates, the latter is not the case. The 2nd pass samples fracture at smaller deformations than the 1st pass sample, but the 3 and 4 pass samples have significantly, although more scattered, larger strain results.

When comparing the original materials used in creating the preforms, the copper sheets exhibit clear signs of softening. Four months of storage at room temperature yields a material that has 14 MPa reduced tensile strength. This is consistent with the recrystallization behavior described in chapter 2.5.1. The aluminum has high strength and low ductility typical for a material with a high degree of cold working. Annealing of the brass sheets gave decreased strength and increased ductility. The high ductility of the “non-annealed” sheets indicate that they may have been annealed after rolling at the factory, being of O- or OS-designation, not H- as presumed. The only effect of the annealing during this investigation would then be grain growth, not recrystallization.

5.3 Flexural tests

The main difference between the Al/Al/Al bend test specimens and the bimetallic materials is that the flexural strength of the sheets does not vary significantly with the number of ARB passes for the aluminum laminate. The strength variations of the bimetallic sheets must be caused by stresses due to difference in plastic flow between Cu/brass and Al, in addition to the obvious strength reduction when the harder layers rupture and become discontinuous. Since the aluminum samples all have increasing degree of cold working, this could mean that for bending purposes of these samples, the bimetallic flow differences are the only factor determining strengthening, not the amount of cold working. However, the increase in cold worked strain seems to have an impact on the total deflection the aluminum laminate is deformed to before failure, although this could be caused by lost plastic flow flexibility due to increased number of roll bonded interfaces as well.

When comparing the cold rolled Al/Cu/Al bend test results to the tensile test, the same trend is observed. The strength increases for the first four passes, and is slightly reduced when necking and fracturing of the copper layers initiate during the 5th pass of accumulative roll

bonding. The layers are deformed along the undulating lines in the material, but the continuity is retained, adding strength to the material in both tensile and flexural stress states.

The brass specimens reach a maximum flexural strength at 3 passes ARB, with declining strength for the 4 pass samples. Unlike the tensile test samples, the annealed 3 pass sheets exhibit no flexural strength decrease compared to the 2nd pass samples. The necking of the brass layers does not seem to affect the strength in bending direction. However, the increased stress field concentrated around a neck could stabilize the material in the normal direction during bend deformation. As soon as the harder brass layers fracture, the flexural strength drops for both brass parallels.

5.4 EBSD images

The EBSD investigations uncovered clear signs of shear band formation in the copper layers. These may be the cause of the undulations observed in the light optical micrographs, and must be considered as an additional instability mechanism contributing to layer fracturing in addition to classical necking.

5.5 Instability mechanisms

In addition to differences in plastic flow and classical necking, formation of shear bands and shear deformation must be considered as an instability mechanism contributing to the deformation and failure of the copper/brass layers. The undulating lines following a seemingly periodic wave line of deformation across layers (Fig. 4.3 e), 4.4 d), and 4.5 e)) is hard to explain with classical necking only. Since occurrences of both mechanisms are observed, it is safe to assume that each of them contribute to the rapid failure of the copper/brass layers. However, the current results seem inadequate for concluding upon the magnitude of each instability mechanism, and which mechanism is the dominant one at the point of layer fracture.

6 Conclusion

When the initial thickness ratio, H , of copper to the total thickness of the metallic multilayered composite is 0.5, the coherency of the copper layers is retained at a number of 6 passes of ARB, when hot rolling, but not for H -value of 0.33. Preforms consisting of one Al and one Cu sheet showed increasing strength with repeated cycles of hot roll bonding, and one Cu sheet between two Al sheets did not show a similar increase in strength.

Similar roll bonding at room temperature leads to premature cracking of both the harder Cu/brass layers, and then the whole specimen during further rolling. This is assumed to be caused by major differences in work hardening rates and plastic flow of the bimetallic systems. Furthermore, periodic, wave-like deformation patterns and formation of shear bands have been observed, leading to the conclusion that shear deformation in the copper/brass layers may contribute to the fracture of these layers at a relatively low number of ARB passes. This leads to the conclusion that shear instabilities have to be considered in addition to classical necking and instabilities due to strain and corresponding plastic flow.

With the materials and preform stacks covered in this work, the amount of passes of cold roll bonding is strictly limited, with failure after 4 passes of cold rolling (in addition to the 1st pass at 350°C). To enable further cycles of ARB, intermediate annealing of the laminate sheets would be required.

7 References

- 1: Eizadjou, A. Kazemi Talachi, H. Danesh Manesh, H. Shakur Shahabi, K. Janghorban: "*Investigation of structure and mechanical properties of multi-layered Al/Cu composite produced by accumulative roll bonding (ARB) process*", Composites Science and Technology, 2008.
- 2: Lee, Bup-Ro Lee, Suk-Bong Kang: "*Control of layer continuity in metallic multilayers produced by deformation synthesis method*", Materials Science and Engineering A 406, p 95-101, 2005.
- 3: Jonsson: "*Mechanical Properties of Metals and Dislocation Theory from an Engineer's Perspective*", Royal Institute of Technology, Sweden, 2010.
- 4: Askeland: "*The Science and Engineering of Materials*", 3rd ed., Nelson Thornes, 1996.
- 5: Vaidyanath, M. G. Nicholas and D. R. Milner: "*Pressure Welding By Rolling*", British Weld Journal, p 13-28, 1959.
- 6: Vaidyanath and D. R. Milner: "*Significance of Surface Preparation in Cold Pressure Welding*", British Weld Journal, p 1-6, 1960.
- 7: Liu, B. Zhang and G.P. Zhang: "*Delaying premature local necking of high-strength Cu: A potential way to enhance plasticity*", Scripta Materiala 64, p. 13-16, 2011.
- 8: Tsuji, Yoshihiro Saito, Seong-Hee Lee, and Yoritoshi Minamino: "*ARB (Accumulative Roll-Bonding) and other new techniques to produce bulk ultrafine grained materials*", Advanced Engineering Materials 5, p 338-344, 2003.
- 9: Matweb.com, data sheets for "*Copper, Cu; Annealed*" and "*Low brass, UNS C24000, OSO25 Temper flat products*".
- 10: Smithells, Brandes E A, Brook G B: "*Smithells light metals handbook*", Elsevier ltd, 1998.
- 11: Kuo, C-S Lin: "*Static recovery activation energy of pure copper at room temperature*", Scripta Materiala 57, p. 667–670, 2007.
- 12: Davis: "*Metals Handbook Desk Edition*", 2nd ed., ASM International, 1998.
- 13: ASM International: "*ASM Metal Reference Book*", Second ed., 1983.
- 14: Haaland: "*Development in mechanical and microstructural properties during deformation and annealing of accumulated roll-bonded aluminium alloys*", p. 52, Master's thesis, Norwegian University of Science and Technology (NTNU), 2007.
- 15: Halmos: "*Roll Forming Handbook*", p. 6-7, 6-8, 6-9, CRC Press, 2006.

Appendix A: Measured thicknesses of the machined samples

Table A.1: Measured thicknesses in mm of the tensile test samples.

Number of passes	1	2	3	4	5
Cold Al/Cu/Al	1.1	1.24	1.3	1.33	1.19
NA Al/brass/Al	1.04	1.33	1.37	1.31	
A Al/brass/Al	1.17	1.3	1.32	1.32	
Al/Al/Al	1	1.09	1.11	1.14	

Table A.2: Measured thicknesses in mm of the flexural test samples.

Number of passes	1	2	3	4	5
Cold Al/Cu/Al	1.1	0.98	1.28	1.32	1.2
NA Al/brass/Al	1.09	1.3	1.4	1.4	
A Al/brass/Al	1.2	1.32	1.35	1.35	
Al/Al/Al	1.03	1.09	1.13	1.13	

The deviations in thickness from specimens of equal number of passes, when comparing tensile test samples with bend test samples, are a result of slight thickness variations across rolled specimens. In addition, some of the samples are taken from two different specimens that were identically treated, but subject to variations of practical nature.